DEPARTMENT OF ELECTRICAL AND ELECTRONIC ENGINEERING

COMMUNICATION AND SIGNAL PROCESSING

Resource Allocation in Wireless Ad-Hoc Networks

Xiaoqin Wang

Master Thesis

September 2011

Supervisor: Dr. Mustafa Gurcan

Abstract

A wireless Ad-Hoc network is an infrastructure-less communication networks without any central administrations, in which nodes communicate with each other utilizing multi-hop wireless links. Intermediate nodes between a pair of nodes that are not in the transmission range of each other act as relays. However, the intermediate nodes along the multi-hop path can drain the battery power of nodes quickly. Therefore, the resource allocation plays a very significant role in dealing with the energy constraint in wireless Ad-Hoc networks. This thesis studies channel-aware resource allocation schemes for High Speed Downlink Packet Access (HSDPA) systems and focuses on the cross-layer resource allocation schemes in wireless Ad-Hoc networks which adopt HSDPA system for communication on each wireless link.

This thesis addresses the problem of the residual transmission energy in HSDPA systems at the physical layer. And a two-group resource allocation scheme is introduced to improve the residual energy utilization. This proposed scheme is examined can achieved a higher data rate than the data rate achieved with the current HSDPA type of algorithm in both interference-free and interference-present environments.

After the transmission power and the data rates are defined as the cost function of the routing scheme, several energy-ware routing path discovery schemes are proposed to find the routing path with the minimum energy consumption. And a novel energy-aware routing path discovery scheme is developed to reduce the computational complexity. As the two-group resource allocation scheme can further reduce the energy consumption per bit for transmission on each path, the data bits can be assigned to each path in such a way that the total energy consumed is minimized. And then, the MAC distributed coordination function (DCF) service time is studied, and the end-to-end delay time of the paths adopting different resource allocation schemes are determined.

Finally, this thesis studies the coded parity packet (CPP) scheme which can decrease the packet error rate and reduce the number of re-transmissions. After the performance of the CPP approach in wireless Ad-Hoc networks is analysed, an adaptable transmission mechanism is developed in this thesis by using CPP scheme to achieve the energy efficiency transmission in wireless Ad-Hoc networks.

Contents

List of Figures

Abbreviations and Acronyms

CDMA	Code Division Multiple Access
UMTS	Universal Mobile Telecommunications System
WCDMA	Wideband Code Division Multiple Access
DS-CDMA	Direct-Sequence Code Division Multiple Access
QoS	Quality of Service
HSDPA	High Speed Downlink Packet Access
3GPP	3rd Generation Partnership Project
DSDV	Destination-Sequenced Distance-Vector Routing
OLSR	Optimized link-state routing protocol
AODV	Ad hoc On-Demand Distance Vector Routing
DSR	Dynamic Source Routing
TORA	Temporally-Ordered Routing Algorithm
SENCAST	Scalable Protocol for Unicasting and Multicasting in a Large Ad hoc Emergency Network
RREQ	Route request packet
AMC	Adaptive Modulation and Coding
QAM	Quadratic Amplitude Modulation
SINR	Signal to Interference plus Noise Ratio
ISI	Inter Symbol Interference
MMSE	Minimum Mean Square Error
SIC	Successive Interference Cancellation
LLR	Logarithm of the likelihood ratio
MAI	Multiple Access Interference

List of Notation

$\vec{a}$	Column vector
$\mathbf{A}$	Matrix
$[\mathbf{A}]_{ij}$	The element of matrix A in row i column j
$\mathbf{A}^{H}$	Conjugate transpose of matrix A
$\mathbf{A}^{T}$	Transpose of matrix A
$\mathbf{A}^{-1}$	Inverse matrix of matrix A
tr($\mathbf{A}$)	trace of matrix A
$\mathbf{A} \otimes \mathbf{B}$	Kronecker product of matrices
$\mathbf{I}_m$	Identity matrix with size m × m
$\lfloor x \rfloor$	The largest integer being smaller or equal to x
$\lceil x \rceil$	The smallest integer being larger or equal to x
$diag(\vec{a})$	The diagonal matrix having the elements of vector $\vec{a}$ in main diagonal line

Acknowledgements

I here confirm that all the technical contributions presented in this thesis are originated in my research, and I will take full responsibilities on them. I also confirm that all the work of others presented in this thesis have been clearly acknowledged and properly cited.

I am most indebted to Dr Mustafa Gurcan, my supervisor, who, in the past few months, introduced me to the HSDPA system and wireless Ad-Hoc networks. His wide knowledge and insightful thinking have been of great value for me. I am thankful for his patience and guidance. It is implausible that I would have seen this endeavour through to its end without him.

I wish also to express my thanks to Mr Anusorn Chungtragarn who gave me useful help during many technical discussions in doing this research.

Finally, above all, I wish to thank my parents. They gave me this opportunity of studying abroad to accept high quality education, and they never ask me to requite for what they have done in the last 23 years. To them I dedicate this thesis.

Chapter 1

Introduction

Wireless Ad-Hoc networks have been the topic of extensive research for around twenty years. Due to their inherent distributed nature, ad-hoc networks are more robust than their cellular counterparts against single-point failure, and have the flexibility to reroute around congested nodes [1]. With limited energy in each node, how to reduce the energy consumption of nodes to transmit a certain amount of data becomes a main research area for wireless Ad-Hoc networks. And the energy consumption is a key design criterion, especially when parallel channel transmission is adopted in these networks. The current high speed downlink packet access (HSDPA) systems with multiple parallel channels, which may produce a significant amount of residual energy for realizing equal data rate per channel, is implemented on wireless Ad-Hoc networks to achieve higher transmission rates.

1.1 Wireless Ad-Hoc Networks

Wireless networks are traditionally classified into two categories: networks with fixed infrastructure and Ad-Hoc networks. The former networks usually comprise one or more centralised nodes which link with the Internet backbone. Mobile nodes can communicate with the access point performing the key networking and control functions for them. There are no peer-to-peer communications between mobile nodes in these networks. And all the mobile nodes can communicate with Internet backbone through the access point by single-hop routing.

A wireless Ad-Hoc network is a collection of nodes which communicate with each other by forming a multi-hop radio network with no centralized administration or fixed infrastructure. The communications between mobile nodes in these networks do not rely on a centralize station/ pre-existing infrastructure to control or coordinate. The nodes in wireless Ad-Hoc networks can communicate directly with each other whenever they are within their transmission ranges and communicate through intermediate nodes using multi-hop routing to

extend their communication ranges and consequently forward their information packets to other nodes which are out of their transmission ranges [2]. An example of a simple Ad-Hoc network is shown in Figure 1.1.

The earliest wireless ad-hoc networks were the “packet radio” networks (PRNETs) dating to the 1970s which is sponsored by DARPA after the ALOHAnet project [3] Wireless Ad hoc networks have been greatly developed in the last forty years and can be further classified into three categories: mobile ad hoc networks (MANETs), wireless mesh networks (WMN) and wireless sensor networks (WSN).

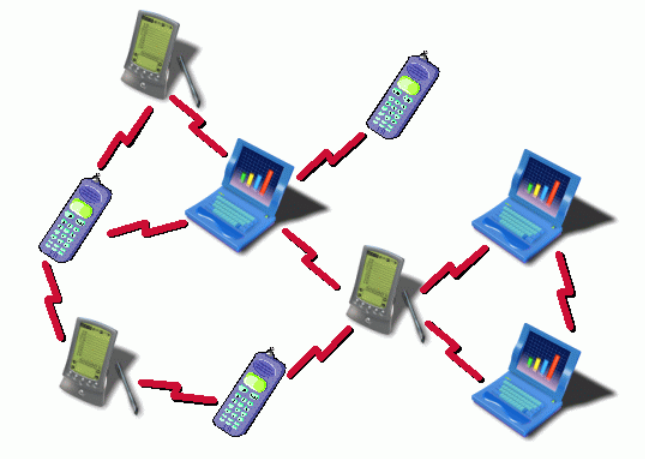

Figure 1.1 A Wireless Ad-Hoc Network

1.2 Routing Protocols in Wireless Ad-Hoc Networks

According to the working principles, the routing protocols in ad-hoc networks can be classified into two categories, one is active routing protocol, and the other is on-demand routing protocol. The active routing protocol maintains fresh lists of destinations and their routes by distributing routing table throughout the network periodically. The typical active routing protocols are DSDV [4], OLSR [5], etc. On the other hand, the on-demand routing protocol, which includes AODV [6], DSR [7], SENCAST [8] does not require routing maintenance. In such protocol, a routing path between the source and the destination is constructed by route discovery when it is demanded. And the contents of the routing tables are only a part of the whole topology of the network. AODV is one of the most popular single-path reactive routing protocols. This protocol establishes route between nodes only as desired by source node. When the source node wants to send packet to destination, it checks the local routing table firstly, and then directly sends the packet to it. Otherwise, the route

request packet (RREQ) is broadcasted by the source node to initiate the process of route discovery. The route reply packet is sent back, if the destination or the intermediate nodes which have route paths to the destination receive the RREQ [6]. When any intermediate node finds its next hop unreachable during the packets transmission, it will send route error packet to the source. And the route discovery process will be initiated again. The appliance of flooding broadcast RREQ is taken in the route discovery process, each node receiving the RREQ should transmit it to its neighbours until the packet have been received by the whole network or part of it [9]. And a reverse route to the source is generated by each node receiving the message.

As the energy constraint is not considered, the weakness of AODV is obvious. The energy of the nodes will be used excessively on receiving and transmitting the duplicate RREQ to different neighbours repeat and frequently. Moreover, the routes in AODV protocol are established based on minimum hop counts. As there is a trade-off between the hop distance and the hop count, the path with minimum hop is usually not the path with the optimal energy consumption. If the same paths are being utilized repeatedly due to the minimum number of route, the nodes energy along these routes will be consumed quickly and may cause the topology partitioned earlier as in the classical routing protocols [10]. And this consideration would cause a bad effect on network lifetime and connectivity when number of nodes increases. To this end, mechanisms which consider the energy consumption of mobile nodes when making routing decisions should be developed. And a lot of research has been done to improve the energy efficiency of ad-hoc wireless network. Several ad hoc routing algorithms such as Dynamic Source Routing (DSR), Ad-hoc On-Demand Distance Vector Routing (AODV), Temporally-Ordered Routing (TORA) and Destination Sequenced Distance vector (DSDV) have been evaluated and analysed in term of their energy consumption [12].

1.3 Propagation Models

In wireless communication, the propagation loss affects the QoS of the links significantly. Basic propagation mechanisms include attenuation, reflection, diffraction and scattering, etc. Numerous of radio propagation models have been developed to estimate the propagation loss of a wireless channel between the transmitter and the receiver. These propagation models can

be divided into two main categories: empirical models and statistic models [13]. Two basic propagation models are introduced and presented below.

1.3.1 Free Space Propagation Model

Free Space indicates that the propagation path between the transmitter and the receiver is a clear, unobstructed line-of-sight. The free space propagation loss is caused by the transmitting signal propagating in every direction all around and the density of power decreases while the distance increases [14]. The receiving power depending on distance and influenced by signal wavelength can be found from the Friis free space equation as follows.

$$P_r = \frac{P_t G_t G_r \lambda^2}{(4\pi d)^2 L_s} \tag{1.1}$$

where P_t is the transmission power, P_r is the receiving power, G_r and G_t are the antenna gains at receiver and transmitter respectively, d is the propagation distance, λ is the radio wavelength, and L_s is the system loss.

1.3.2 Two-Ray Ground Reflection Model

A single line-of-sight path is rarely the only propagation path between the transmitter and the receiver in practical cases which makes the results of free space propagation model inaccurate. Therefore, a model which considers both the direct path and a ground reflection path is introduced. It is shown [14] that this Two-Ray Ground reflection model provides more accurate estimation at a long distance than free space model. The received power at distance d can be predicted according to the equation below.

$$P_r = \frac{P_t G_t G_r {h_t}^2 {h_r}^2}{d^4 L_s} \tag{1.2}$$

where h_t and h_r are the heights of the transmitting and receiving antennas respectively.

1.4 HSDPA Overview

The 3rd Generation Partnership Project (3GPP) is the forum where standardization is handled for HSDPA and HSUPA and has been handled from the wideband code division multiple access (WCDMA) specification release as well [15]. In order to improve the efficiency of the spectrum utilization, DS-CDMA channel access method multiplexes sub-stream of raw

information bits in WCDMA air interference by modulating the transmitted signals in each sub-stream utilizing a unique sequence of chips [15]. And each chip has much shorter duration than the information bit.

Based on the WCDMA air interface, high speed data packet access (HSDPA) is developed. As this packet-based data service enhances the performance of the WCDMA in 3G communication systems, HSDPA is also known as the 3.5G mobile communication systems. HSDPA is one of the members in High-Speed Packet Access (HSPA) family. Current HSDPA deployments support down-link speeds of 1.8, 3.6, 7.2 and 14.0 Megabit/s. Further speed increases are available with HSPA+, which provides speeds of up to 42 Mbit/s downlink and 84 Mbit/s with Release 9 of the 3GPP standards [16].

HSDPA introduced a new transport channel—High-Speed Downlink Shared Channel (HS-DSCH) which is dedicated for high-speed data transmission. Channel-dependent scheduling is adopted to facilitate air interface channel-sharing between clients. It comprises three newly introduced physical layer channels: High Speed-Shared Control Channel (HS-SCCH); the High Speed-Dedicated Physical Control Channel (HS-DPCCH); and the High Speed- Physical Downlink Shared Channel (HS-PDSCH).

In HSDPA systems, K=5, 10 or 15 spreading codes which use the same QPSK and MQAM modulation schemes are adopted for one single user to implement multi-channel data transmission [17]. Adaptive modulation and coding (AMC) technique, which allows the modulation and coding schemes can be changed according to the signal quality for individual users, is used to replace the power control functions in WCDMA and can significantly increase the downlink capacity. Moreover, hybrid automatic repeat-request (HARQ) [17], a fast physical layer-based retransmission mechanism, is used in HSDPA system to reduce latency and improve the roundtrip time.

The HSDPA model, which is constructed based on the HSDPA protocol in 3GPP Release 5, is used in the thesis and presented in Chapter 2. In this model, all available physical layer channels are assumed to be dedicated to one single user. AMC mechanism is implemented to adjust transmission bit rate for each channel according to the signal quality, which can explore the optimum solutions on allocating bits and powers in multi-channels.

1.5 Thesis Outline

The following chapters of the thesis are organized as follows. In Chapter 2, the structure of the HSDPA system is first studied and introduced. Then, the energy utilization problem is then presented and analysed in HSDPA systems, and related residual energy and achievable data rate are addressed and tested. In order to solve the problem of the inefficient energy utilization in HSDPA systems, a two-group resource allocation scheme [18] which assigns the information bits into two groups of channels with different numbers of bits per symbol are adopted and analysed carefully. At last, the related work on the MAC DCF study is reviewed and the MAC DCF service time is studied from analysing and examining a DCF model which is developed in [19] for multi-hop wireless Ad-Hoc networks. In Chapter 3, the energy utilization problem for routing scheme in multi-rate networks is addressed. And energy consumption of each hop along a routing path forms the core part of the cost function. A trellis-hop diagram approach is presented to find all the possible routing paths of a given node pair in a network. And a modified Viterbi solution [20] [21] is introduced to reduce the computational complexity of trellis diagram approach. Moreover, in order to reduce the computational complexity of discovering the best paths between every two nodes in a network, a modified Floyd's algorithm is developed. In Chapter 4, the coded parity packets approach [22] [23] is studied and analysed. Then based on CPP approach, an adaptable transmission mechanism is developed to improve the energy efficiency in wireless Ad-Hoc networks. Finally, the summary of this thesis is provided in Chapter 5, and some future works are outlined.

Chapter 2

Two Group Resource Allocation Scheme and MAC DCF Service Time

2.1 Introduction

In this chapter, the HSDPA system used for a single link between two nodes in the wireless Ad-Hoc Networks is introduced. Moreover, the resource allocation schemes which can optimum the transmission rate under certain transmission energy are studied and analysed. Finally, a MAC layer model of wireless Ad-Hoc networks, which is adopted in this project, is presented.

2.2 High-Speed Downlink Packet Access (HSDPA) System

In this section, a simple HSDPA system is introduced to present the whole signal processing. The whole signal processing procedure can be divided into three stages: signal processing at the transmitter, the channel and the signal processing at the receiver. In Figure 2.1, the procedures of the signal processing in continuous time and discrete time domain are presented for one sub-channel in HSDPA systems.

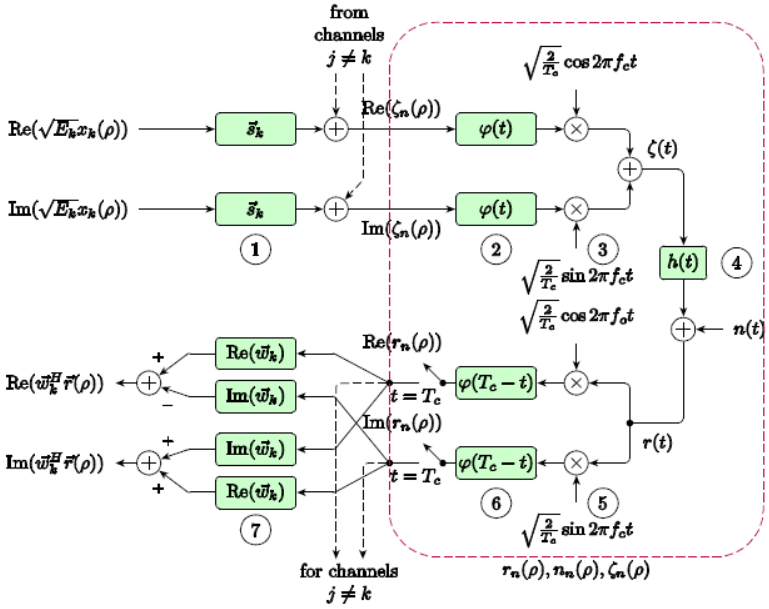

Figure 2.1 Signal processing and transmission in discrete time and continuous time domains for a single sub-channel

2.2.1 Signal Processing at the Transmitter

In *k-th* sub-channel, the coded binary bit stream is passed to the modulation unit and mapped into symbols b_k. then the channel symbol b_k is scaled to $\sqrt{E_k}b_k$ where E_k is the allocation energy per symbol. After power control procedure, the generated and scaled complex-valued channel symbol, $\sqrt{E_k}b_k$ for *k-th* sub-channel, first separates its real and imaginary components into two branches, the I (upper) branch and the Q (lower) branch, respectively [15]. Following on from that, a spreading filter processes on channel symbol components in both branches. The spreading filter is represented by an *N*-length vector $\overline{s_k}$. A series of *N* chips with one chip duration $T_c = T_s/N$ is generated. Then each chip in both branches is multiplied with a common chip pulse-shaping function $\varphi(t)$ to transform the discrete time signals in chips to continuous time waveforms [15]. The transmitter will then transmit the continuous time waveform in the radio channel after the waveform has been modulated to the carrier frequency f_c.

2.2.2 Radio Channel

The loss in the radio channel with a certain propagation distance and carrier frequency can be estimated by various propagation models. For instance, if the channel is non-frequency

selective, the amplitude of the received signal can be expressed as $A_k = \sqrt{h_k E_k}$, where h_k is the channel gain for *k-th* sub-channel. At the input of the receiver, received signals are corrupted by the noise and MAI, and are presented as $r_k = \sqrt{h_k E_k} b_k s_k + I_{MAI} + I_n$, where I_{MAI} is the MAI factor and I_n is the noise [24].

2.2.3 Signal Processing at the Receiver

At the receiver, the received waveform is the convolution of the transmitted waveform $\zeta(t)$ with the channel impulse response *h(t)* pulsing the additive white noise *n(t).* Firstly, the received waveform is demodulated by two demodulation functions with a π/2 shift to baseband signals which separate the real components and imaginary components. Then the chip-match function $\varphi(T_c - t)$ is performed to convolve with the signal in both I and Q branch respectively, and the output is sampled in every T_c seconds. A common filter, represented by the vector $\overline{w_k}$, then operates on the I and Q branches of signals $r_n(\rho)$ to despread the channel symbol estimation in every n chips. After the dispreading procedure, the signal is demapped from symbols to bit streams.

2.3 Rate Allocation in HSDPA Systems

Figure 2.2 illustrates a simplified discrete-time model for HSDPA system with frequency selective channel, in which the I and Q branches are combined. There are *K* sub-channels in this HSDPA system. And the information bits are demultiplexed into *K* substreams in the base station. In *k-th* substream, the information bits are encoded and modulated to complex symbols, b_k, in each T_s seconds. In AMC Units, the amount of information bits in each symbol for each coded channel is determined. And in Power Units, the channel symbols are scaled to $E_k(b_k) = \sqrt{E_k} b_k$ with E_k is the allocated energy per symbol in *k-th* sub-channel. Then the symbols are passed through the spreading filters $\vec{s}_k$ which is different for each channel to generate a series of *N* chips per symbol. *N* is named as the processing gain. Then the chips of *K* sub-channels are added together and sent. At the receiver end, the depreading sequences are adopted to minimize the cross-correlations from the noise and the other coded channels. Then the information bits in each coded channel are retrieved from the output of the depreading filters.

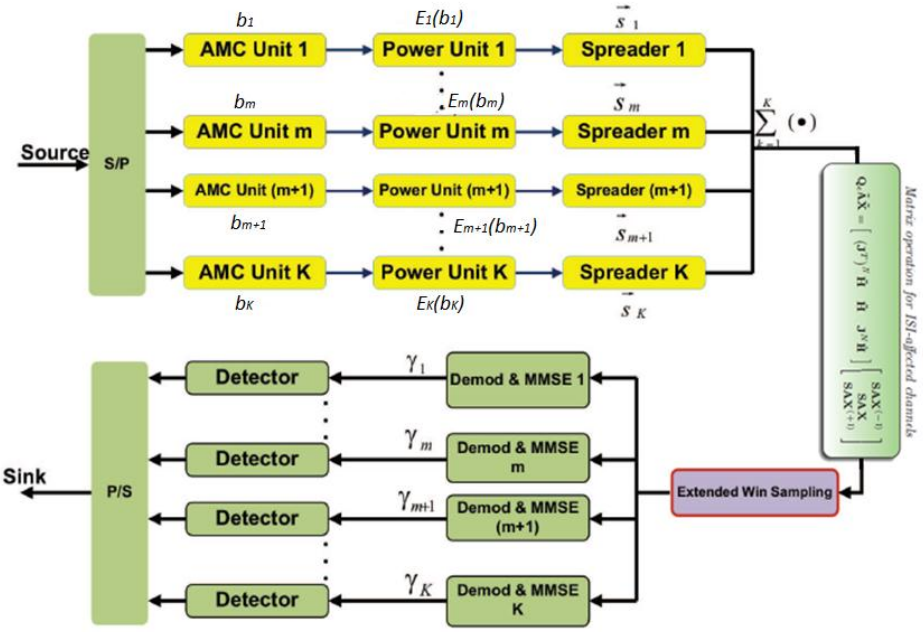

Figure 2.2 HSDPA System Structure

2.3.1 Equal Energy and Equal Rate Allocation in HSDPA Systems

Equal energy and equal rate allocation scheme is a method which constraints the powers and bit rates be to assigned uniformly among all used sub-channels while varying the number of active sub-channels to achieve the maximum total bit rate.

Consider a wireless link employing multi-code HSDPA with a processing gain of N_{PG} for *K* physical layer sub-channel, each channel of which adopts a unique spreading sequence, hence the *K* sub-channels are orthogonal to each other. The transmitted data can be adaptively loaded using AMC at P different rates of

$$b_p = \beta p \tag{2.1}$$

where β represents the incremental amount between any two adjoining bit rate values, which is named as bit granularity in this thesis. It is defined as $\beta = b_p - b_{p-1}$ for $p=1,2,\ldots,P$. The transmitted energy per symbol per channel to achieve the transmission the bit rate b_p can be expressed as

$$E(b_p) = \frac{2\sigma_n^2\Gamma}{|h|^2}(2^{b_p} - 1) \quad p=1, 2\ldots P \tag{2.2}$$

where *h* is the amplitude attenuation factor for an interference-free channel, Γ is the gap value which illustrates the performance difference between the practical modulations and coding

schemes with the optimal cases, and $2\sigma_n^2$ is the noise samples variance at the output of the chip-match filter.

In order to accomplish the equal rate allocation in *K* active sub-channels, the total available energy is allocated to *K* parallel channels equally. As it is assumed that the channels are non-frequency selective, the SNR are the same at the input of *K* channels. As the sum of the energy transmitted in *K* parallel channels to provide bit rate b_p in each channel, cannot exceed the given transmission energy E_T. We have $KE(b_p) \leq E_T$. And related SNR for each channel satisfies$SNR(b_p) \leq \frac{SNR_T}{K}$, where SNR_T and $\text{SNR}(b_p)$ can be found from

$$SNR_T = \frac{|h|^2 E_T}{2\sigma_n^2} \tag{2.3}$$

$$SNR(b_p) = \frac{|h|^2 E(b_p)}{2\sigma_n^2} \tag{2.4}$$

According to the equations above, the bit rate per symbol per channel b_p can be expressed as follows.

$$b_p = log_2(\frac{SNR(b_p)}{\Gamma} + 1) \tag{2.5}$$

$$b_p \leq log_2(\frac{SNR_T}{\Gamma K} + 1) \tag{2.6}$$

Therefore, the equal rate and power method can achieve the maximum total bit rate as follow.

$$\max(R_T) = Kb_p \tag{2.7}$$

where *K* is the number of active parallel channels which can be chosen from 1 to 15.

2.3.2 Residual Energy Utilization

In the previous section, the equal energy allocation is introduced. However, this approach results in a considerable amount of residual energy which is not adopted to transmit any useful information. This residual energy is defined as below.

$$e_R = E_T - KE(b_p) < K\left(E_k(b_{p+1}) - E_k(b_p)\right) = Ke(b_p) \tag{2.8}$$

where $e(b_p)$ is the incremental energy. The incremental energy to realize an additional data rate of β bits per symbol from a lower data rate of b_p to b_{p+1} is defined as

$$e(b_p) = E_k(b_{p+1}) - E_k(b_p) = \frac{2\Gamma\sigma^2}{|h|^2}(2^{\beta} - 1)2^{b_p} \tag{2.9}$$

According to equation (2.8) and (2.9), when the equal rate allocation scheme is adopted in multi-code HSDPA systems, an inefficient usage of the limited available energy, which usually results in reducing the total data rate in HSDPA system, is raised.

2.3.3 Two-group Resource Allocation Scheme

In a multi-code HSDPA system, the residual energy mentioned above can be very significant sometimes. In order to better use the residual energy and increase the transmission data rate, some of the residual energy can be utilize to load a number of channels with a higher data rate [25]. After equal rate algorithm operates on finding data rate b_p per symbol for every sub-channel, there are m channels which can utilize the residual energy to achieve b_{p+1} bits per symbol. And the rest of the channels are loaded with b_p. The overall energy E_T satisfies the following inequality:

$$E^{(m)}(b_p) \leq E_T < E^{(m+1)}(b_p), \tag{2.10}$$

where

$$E^{(m)}(b_p) = mE_k(b_{p+1}) + (K - m)E_k(b_p), \tag{2.11}$$

$$E^{(m+1)}(b_p) = (m + 1)E_k(b_{p+1}) + (K - m - 1)E_k(b_p). \tag{2.12}$$

The whole process is illustrated below. In Figure 2.3, $e_k(b_p)$ represents the incremental energy to transmit bit rate from b_p to b_{p-1} in *k-th* sub-channel.

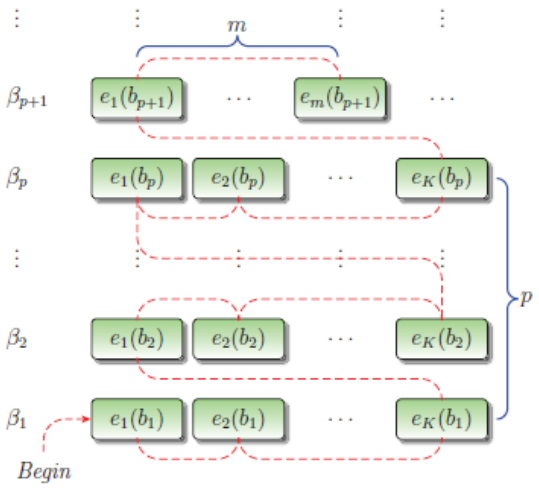

Figure 2.3 Procedure of bit channel loading for the Two Group algorithm

The maximums overall bit rate is acquired as:

$$R_T = (K - m)b_p + mb_{p+1} \tag{2.13}$$

which indicates the overall data rate is maximized when the bit rate b_p is allocated to *K-m* channels, and the bit rate b_{p+1} is allocated to m channels. This joint allocation of bit rates and transmission energy is named as two-group resource allocation scheme, in which the channels loading bit rate b_p are low-rate channels, while the channels loading b_{p+1} are called high-rate channels [25].

Under the same assumptions made above and By knowing a given set of parameters which include h, σ^2, Γ, β and E_T, as well as a set of discrete bit rate values $\{b_p\}_{p=1}^{P}$, the bit rate index p for the low-rate channels can be derived as

$$p = \min\left(\left\lfloor \frac{log_2\left(1+\frac{E_T|h|^2}{K(2\sigma_n^2)\Gamma}\right)}{\beta} \right\rfloor, P\right) \tag{2.14}$$

After obtain the value of p, the number of high-rate channels which loading with bit rate b_{p+1} can then be determined as

$$m = \left\lfloor \frac{E_T - KE_k(b_p)}{E(b_{p+1}) - E(b_p)} \right\rfloor \tag{2.15}$$

After the lower data rate index p is derived from equation (2.14) and the number of higher data rate channel m is computed from equation (2.15), the transmission process can operate by transmitting b_p bits per symbol in *K-m* sub-channels while transmitting b_{p+1} bits per symbol in the other m channels.

2.3.4 Resource Allocation in Frequency Selective Channels

When the multi-code HSDPA system operates over an environment with multipath propagation feature and the wireless link is rather frequency selective than flat, the signature sequences in parallel channels become non-orthogonal at the receiver end, and channels are interfered by signals in the other channels and in other symbol periods. For the channels with interference, two-group resource allocation scheme can implemented to achieve the maximum overall transmission bit rate as well.

Consider a HSDPA system with frequency selective channels, the data is passed through the serial to parallel encoder first in which information are separate into *K* blocks. The orthogonal signature sequences are given by

$$\boldsymbol{S} = [\overrightarrow{s_1},\ \overrightarrow{s_2}, \dots ,\ \overrightarrow{s_K}]. \tag{2.16}$$

A discrete time channel impulse vector is used for the frequency selective channel with *L* propagation paths.

$$\vec{h} = [h_0, h_1, \dots, h_{L-1}]^T \tag{2.17}$$

where h_l is the channel coefficient of *l-th* path with a time delay l chip periods. In every symbol period, the frequency selective channel is assumed can be characterized by the *(N+L-1)×N* channel convolution matrix:

$$\mathbf{H} = \begin{bmatrix} h_0 & 0 & \cdots & 0 \\ \vdots & h_0 & & \vdots \\ h_{L-1} & \vdots & \ddots & 0 \\ 0 & h_{L-1} & & h_0 \\ \vdots & \vdots & \ddots & \vdots \\ 0 & 0 & \cdots & h_{L-1} \end{bmatrix}$$

The interference is caused by the non-zero entries in matrix **H** except h_0. Due to the channel interference, the received signal at the match filter given by

$$Q = [\overrightarrow{q_1},\ \overrightarrow{q_2}, \dots, \overrightarrow{q_K}] = [0^T_{\alpha\times K}, (\boldsymbol{HS})^T, 0^T_{(\alpha-L+1)\times K}]^T \tag{2.18}$$

which is not orthogonal anymore. To reduce the interference, a channel equalizer, which is developed on minimum mean square error (MMSE) approach for HSDPA systems, is presented in [26]. In [26], the depreading vectors are given by

$$\overrightarrow{w_k} = \frac{\boldsymbol{C}^{-1}\overrightarrow{q_k}}{\overrightarrow{q_k}\boldsymbol{C}^{-1}\overrightarrow{q_k}}, \tag{2.19}$$

where $\boldsymbol{C}$ is the covariance matrix and is given by

$$\boldsymbol{C} = \boldsymbol{Q}\boldsymbol{A}^2\boldsymbol{Q}^H + 2\sigma^2\boldsymbol{I}_{N+L-1}. \tag{2.20}$$

$\boldsymbol{A}$ is a diagonal matrix which is given by

$$\boldsymbol{A} = diag(\sqrt{E_1}, \sqrt{E_2}, \dots, \sqrt{E_K}), \tag{2.21}$$

where E_k is the transmission energy per symbol period in each channel.

In this case the output SNRs are calculated as follows:

$$\gamma_k = \frac{E_k \overrightarrow{s_k}^H H^H C^{-1} H \overrightarrow{s_k}}{1 - E_k \overrightarrow{s_k}^H H^H C^{-1} H \overrightarrow{s_k}} = \frac{E_k \overrightarrow{q_k}^H C^{-1} \overrightarrow{q_k}}{1 - E_k \overrightarrow{q_k}^H C^{-1} \overrightarrow{q_k}} \tag{2.22}$$

where *k* is the index of the parallel channel from 1 to *K*.

When Inter-symbol Interference is considered, a window extended model presented in [27] is adopted to improve the system performance and total capacity. By extending the window length by α-chip on each side, this window records a part of the next symbol period and a portion of the previous symbol period. The new receiver signature sequence matrix is then given by

$$\tilde{Q} = [(\boldsymbol{J}^T)^N \tilde{\boldsymbol{H}} \boldsymbol{S},\ \tilde{\boldsymbol{H}} \boldsymbol{S},\ \boldsymbol{J}^N \tilde{\boldsymbol{H}} \boldsymbol{S}] \tag{2.23}$$

where

$$\boldsymbol{J}_{N+2\alpha} = \begin{bmatrix} \vec{0}_{1\times(N+2\alpha-1)} & 0 \\ I_{(N+2\alpha-1)} & \vec{0}_{1\times(N+2\alpha-1)} \end{bmatrix} \tag{2.24}$$

And

$$\tilde{\boldsymbol{H}} = [0^T_{\alpha\times K},\ \boldsymbol{H}^T,\ 0^T_{(\alpha-L+1)\times K}]^T. \tag{2.25}$$

On the other hand, the correspond covariance matrix is modified as

$$\tilde{C} = \tilde{\boldsymbol{Q}} \tilde{\boldsymbol{A}}^2 \tilde{\boldsymbol{Q}}^H + 2\sigma^2 \boldsymbol{I}_{N+2\alpha}, \tag{2.26}$$

where $\tilde{A} = I \otimes diag(\sqrt{E_1}, \sqrt{E_2}, \dots, \sqrt{E_K})$.

The whole process of the two-group resource allocation schemes can be divided into two parts such as Equal rate allocation and Residual energy allocation.

Algorithm 1. Equal rate allocation algorithm (finding b_p)

1: Set *j*=1, and initialize $E_k = \frac{E_T}{K}\ for\ k = 1,2, \dots, K$ and initialize the amplitude diagonal matrix

$$\tilde{A} = I \otimes diag(\sqrt{E_1}, \sqrt{E_2}, \dots, \sqrt{E_K})$$

2: Set i=1, y_k=b_j, $\gamma^*(y_k) = \Gamma(2^{y_k} - 1)$ and $\tilde{A}_i = \tilde{A}$ for k=1,2...K

3: Compute the covariance matrix at this stage:

$$C_i = Q_e \tilde{A}_i^2 {Q_e}^H + 2\sigma^2 I_{N+2\alpha}$$

4: Renew the energy $E_{k,i+1}(y_k) = \frac{\gamma^*(y_k)}{(1+\gamma^*(y_k))\vec{q}_k^H C_i^{-1}\vec{q}_k} \quad for\ k = 1,2,\dots,K$

5: Update the amplitude diagonal matrix:

$$\tilde{A}_{i+1} = \boldsymbol{I} \otimes diag(\sqrt{E_{1,i}}, \sqrt{E_{2,i}}, \dots, \sqrt{E_{K,i}})$$

6: Set *i=i+1*

7: If $E_{k,i}(y_k) \neq E_{k,i-1}(y_k)$ for k=1,...,K and $i \leq \mathbf{I}_{\max}$ (for example $\mathbf{I}_{max}$=50) go back to step 3. Otherwise go to the next step.

8: Set j=j+1, $E_{k,temp} = E_{k,i}(y_k)\ for\ k = 1,2,\dots K$ and go to step 2, when *j*<P and $\sum_{k=1}^{K} E_{k,i}(y_k) < E_T$,. Otherwise $E_k = E_{k,temp}$ for k=1,…, K and *p=j-1*. $E_{k,i}(y_k)$ is the allocated energy to achieve the transmission data rate b_p in *k-th* channel.

After the energy of transmitting the data rate b_p bits per symbol is allocated for each channel, the residual energy is given by $E_{resdual} = E_T - \sum_{k=1}^{K} E_k(b_p)$. The residual energy is utilized to transmit b_{p+1} bits per symbol in m channels.

Algorithm 2. Residual energy allocation algorithm (finding *m*)

1: Sort the channels in ascending order, for example the first channel corresponds to the channel $k = \arg min_{k \leq K} (E_k(b_{p+1}) - E_k(b_p))$.

2: Set j=1 and calculate the amplitude diagonal matrix

$$\tilde{A} = I \otimes diag(\sqrt{E_1}, \sqrt{E_2}, \dots, \sqrt{E_K})$$

3: Set i=1, $y_k = b_{p+1}$ for k=1,…,j, $y_k = b_p$ for k=j+1,…,K, $\gamma^*(y_k) = \Gamma_j(2^{y_k} - 1)$ and $\tilde{A}_i = \tilde{A}$ for k=1,2...K.

4: Compute the covariance matrix at this stage:

$$C_i = Q_e \tilde{A}_i^2 {Q_e}^H + 2\sigma^2 I_{N+2\alpha}$$

4: Update the energy $E_{k,i+1}^{(j)}(y_k) = \frac{\gamma^*(y_k)}{(1+\gamma^*(y_k))\vec{q}_k^H C_i^{-1}\vec{q}_k} \quad for\ k = 1,2,\dots,K$

5: Update the amplitude diagonal matrix:

$$\widetilde{\boldsymbol{A}}_{i+1} = I \otimes diag(\sqrt{E_{1,i}}, \sqrt{E_{2,i}}, \dots, \sqrt{E_{K,i}})$$

6: Set *i=i+1*

7: If $E_{k,i}(y_k) \neq E_{k,i-1}(y_k)$ for k=1,...,K and $i \leq I_{\max}$ (for example I_{max}=50) go back to step 4. Otherwise go to the next step.

8: Let j=j+1, $E_{k,temp}^{(j)} = E_{k,i}^{(j)}(y_k)\ \ for\ \ k = 1,2, \ldots K$ and go to step 3, when $\sum_{k=1}^{K} E_{k,i}^{(j)}(y_k) < E_T$ and j<K-1. Otherwise $E_k = E_{k,temp}$ for k=1,…, K and *m=j-1*.

After b_p is determined from Equal rate allocation algorithm and *m* is derived from Residual energy allocation algorithm, the two-group resource allocation scheme is accomplished. And the limited transmission energy is optimal allocated to achieve the maximum bit rate.

2.4 MAC DCF Working Process

The model of wireless ad-hoc network in this thesis is built on IEEE 802.11 distributed coordination function (DCF) to analysis the successful transmission probability, collision probability and maximum service time of the network.

In 802.11 MAC layer, the DCF is defined as the distributed channel access MAC protocol which allows the sharing of the medium channel between nodes in a network. The DCF applies the binary exponential back-off algorithm on nodes to obtain channel access permission, and DCF provides two selections which include a two-way handshaking mechanism and RTS/CTS mechanism to prevent collision from occurring. As RTS/CTS mechanism which provides a better performance on avoiding collision caused by the hidden-terminal problem is described and adopted in this thesis.

In a network, nodes are demanded to listen to the channel state for a DCF Inter Frame Space (DIFS) interval before transmitting [28]. If the channel is sensed to be idle or free during a DIFS interval, the transmitting node is permitted to use the channel for transmissions; otherwise, if the channel is sensed busy during a DIFS interval, the node enters the back-off process and not allowed to transmitting.

When the source node is permitted to transmit packets, a Request-to-Send (RTS) packet will be transmitted first to the destination node. If the RTS packet is successfully received by the destination node, the destination will send a Clear-to-Send (CTS) packet back to the source node to confirm that the destination node is ready to receive the data packet, if the channel is still free. As the RTS/CTS packets contain information about the length of the data packets, the node which receives the packets can be on standby for a certain amount of time interval according to the need for data packets transmissions [24, 28]. If the CTS packet is correctly received by the source node, it then obtains the permission to transmit the data packet. After the data packet is successfully received at the destination node, a corresponding

acknowledgement (ACK) packet will be sent from the destination node to the source node to confirm the reception of the data packet. The Short Inter-Frame Space (SIFS) is used to separate the transmission of all packets which include RTS, CTS, DATA and ACK. SIFSs provide the time for transition between transmitting and receiving of source node and destination node. Figure 2.4 illustrates the process of distributed coordination function.

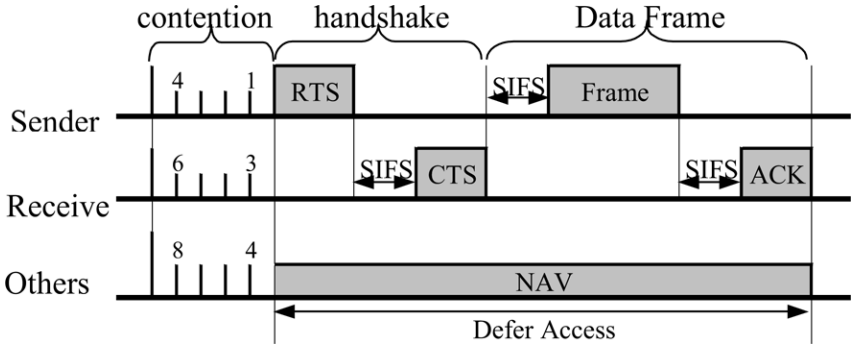

Figure 2.4 DCF Transmission

The time consumed for one full successful transmission, which is defined as the sum of the time consumed for every control packet transmission, data packet transmission and the time intervals, is given by [19]

$$T_s = t_{DIFS} + t_{RTS} + t_{CTS} + 3 \times t_{SIFS} + 4 \times \delta + E\{P\} + t_{ACK} \tag{2.27}$$

where $E\{P\}=L/r_{data}$ is the time consumed for data packet transmission with a packet length L-bit and bit rate r_{data}. t_{DIFS}, t_{RTS}, t_{CTS} and t_{ACK} are the time slots for control packets transmission. These control packets are transmitted at a certain rate in DCF. In this thesis, this rate is chosen as 1 Mb/s. t_{SIFS} is the time interval among the packets transmissions. δ is the propagation delay which is very small.

On the other hand, the time consumed for detecting a collision occurrence is provided below.

$$t_c = t_{RTS} + t_{DIFS} + \delta \tag{2.28}$$

It means that if the destination node does not receive the RTS packet in a time duration t_c, a collision is considered to happen. The detailed parameter values of IEEE 802.11 are provided in Table 1.

Table 1: IEEE 802.11 Simulation Parameters.

MAC		PHY	
$W_{\min}$	32	Temperature (Kelvin)	290
$W_{\max}$	1024	Noise factor	10
MAC Header (bytes)	34	Transmission power (dBm)	10
ACK (bytes)	38	Sensitiviy of PHY (dBm)	-87.039
CTS (bytes)	38	Minimum power for	
RTS (bytes)	44	received packet (dBm)	-76.067
Slot Time (μsec)	20	Packet reception model	BER
SIFS (μsec)	10		
DIFS (μsec)	50		

2.5 MAC DCF Service Time

Marcelo M. Carvalho developed a scalable DCF model [19] for the analytical study of medium access protocol operating in multi-hop wireless Ad-Hoc networks. This model is built by expressing each layer's functionality in probabilistic terms. In the PHY layer, the probability of a successful frame reception is concerned. And in MAC layer, the model is concerned with its scheduling rate.

2.5.1 Successful Frame Reception Probability

Let V represent the finite set of |V|=n nodes which construct the network in this section, and let $V_r \subseteq V$ denote the subset of the nodes whose power can be received at node r below the threshold. When $|V_r|=n_r$ and the frame is transmitted by node i, there are 2^{n_r-1} combinations of active transmitting nodes in subset V_r. And let $\{c_{ik}^r\}_{k=1,2,\ldots,2^{nr-1}}$ represent the set of these combinations.

Provided the considerations above, the probability q_i^r that a frame, which is transmitted by node i, is received at node r successfully can be expressed as follows:

$$\begin{aligned} q_i^r &= P\{successful\ frame\ reception\} \\ &= \sum_k P\{successful\ frame\ reception, C_i^r = c_{ik}^r\} \\ &= \sum_k P\{succ.\ frame\ reception | C_i^r = c_{ik}^r\} P\{\ C_i^r = c_{ik}^r\} \\ &= \sum_k f(c_{ik}^r) P\{C_i^r = c_{ik}^r\} \end{aligned} \tag{2.29}$$

The above formalism allows for the consideration of any radio channel model and PHY-layer aspect for computation of the probability $f(c_{ik}^r)$ of successful frame reception conditioned on a certain MAI level [19]. And the scheduling probability (transmission

probability) of each node is τ_j, $j \in V_r$, which depends on the perceived activity of other nodes. Therefore, $P\{C_i^r = c_{ik}^r\}$ is given by,

$$P\{C_i^r = c_{ik}^r\} = \prod_{m \in \overline{c_{ik}^r}} (1 - \tau_m) \prod_{n \in c_{ik}^r} \tau_n \tag{2.30}$$

where $\overline{c_{ik}^r}$ is the complement set of c_{ik}^r.

Eventually, the successful received probability is given by

$$q_i^r = \sum_k f(c_{ik}^r) \prod_{m \in \overline{c_{ik}^r}} (1 - \tau_m) \prod_{n \in c_{ik}^r} \tau_n \tag{2.31}$$

2.5.2 Scheduling Probability

In reality, at each attempt, two events require to happen for node *i* to consider its frame successfully transmitted to a node *r*: the successful reception of node *i*'s frame at node *r*, and the successful reception of node *r*'s acknowledgement at node *i* [19]. Thus,

$$\begin{aligned} q_i &= P\{DATA\ successful, ACK\ successful\} \\ &= P\{ACK\ succ. | DATA\ succ.\} P\{DATA\ succ.\} \\ &= q_i^r q_r^i = \sum_k f(c_{ik}^r) P\{C_i^r = c_{ik}^r\} \sum_l f\left(c_{rl}^i\right) P\left\{C_r^i = c_{rl}^i\right\} \\ &= \sum_k \sum_l f(c_{ik}^r)\, f\left(c_{rl}^i\right)\, P\{C_i^r = c_{ik}^r\}\, P\left\{C_r^i = c_{rl}^i\right\} \end{aligned} \tag{2.32}$$

The feedback information must be utilized by the MAC protocol to schedule the retransmission which can minimize the unsuccessful transmission times. In this way, the MAC protocols can be treated as a dynamic system with the feedback information q_i and the corresponding output τ_i. The relation between q_i and τ_i can be expressed as follows:

$$\tau_i = h_i(q_i),\ i \in V. \tag{2.33}$$

In this model, the network is assumed to be saturated which indicates a packet is always available for transmission at the head of a node's queue. And a linear relation has been set between successful reception probability and the scheduling rate. We have

$$\boldsymbol{\tau} = a\boldsymbol{q}, \tag{2.34}$$

where a=$\frac{2W_{min}}{(W_{min}+1)^2}$, and W_{min} denotes the minimum window size. And in this model, the situation with no MAI is used to provide an approximation of successful reception probability q_i.

$$q_i = f\left(c_{r0}^i\right) f(c_{i0}^r) \prod_{j\in \mathrm{V_r}}(1-\tau_j) \prod_{j\in \mathrm{V_i}}(1-\tau_k)$$
$$= f\left(c_{r0}^i\right) f(c_{i0}^r) \prod_{j\in \mathrm{V_r}}(1-\mathrm{aq}_j) \prod_{j\in \mathrm{V_i}}(1-\mathrm{aq}_k)$$
$$\approx f\left(c_{r0}^i\right) f(c_{i0}^r) \left(1-\sum_{j\in \mathrm{V_r}\cup \mathrm{V_i}} aq_j\right) \quad (2.35)$$

By making $f\left(c_{r0}^i\right) f(c_{i0}^r) = \pi_i$, and considering the set V with all nodes in the network topology, we have

$$q_1 = \pi_1 - a\pi_1 \sum_{j\in \mathrm{V_{r_1}}\cup \mathrm{V_1}} q_j \quad (2.35)$$

$$q_2 = \pi_2 - a\pi_2 \sum_{j\in \mathrm{V_{r_2}}\cup \mathrm{V_2}} q_j \quad (2.36)$$

$$\vdots$$

$$q_n = \pi_n - a\pi_n \sum_{j\in \mathrm{V_{r_n}}\cup \mathrm{V_n}} q_j \quad (2.37)$$

where r_i denotes the intended receiver of node i. The equations above can be expressed in matrix form.

$$\begin{bmatrix} q_1 \\ q_2 \\ q_3 \\ \vdots \\ q_n \end{bmatrix} = \begin{bmatrix} \pi_1 \\ \pi_2 \\ \pi_3 \\ \vdots \\ \pi_n \end{bmatrix} - \begin{bmatrix} 0 & \phi_{12} & \phi_{13} & \cdots & \phi_{1n} \\ \phi_{21} & 0 & \phi_{23} & \cdots & \phi_{2n} \\ \phi_{31} & \phi_{32} & 0 & \cdots & \phi_{3n} \\ \vdots & \vdots & \vdots & \ddots & \vdots \\ \phi_{n1} & \phi_{n2} & \phi_{n3} & \cdots & 0 \end{bmatrix} \begin{bmatrix} q_1 \\ q_2 \\ q_3 \\ \vdots \\ q_n \end{bmatrix}, \quad (2.38)$$

where

$$\varphi_{ij} = \begin{cases} a\pi_i, & if\ j \in V_i \cup V_{r_i} \\ 0, & if\ j \notin V_i \cup V_{r_i} \end{cases} \quad (2.39)$$

Therefore, the successful transmission probability q_i can be derived from

$$\boldsymbol{q} = (\boldsymbol{I} + \boldsymbol{\Phi})^{-1}\boldsymbol{\pi} \quad (2.40)$$

The probability of successful frame reception conditioned on a certain MAI level can be found from

$$f(c_{i0}^r) = \{1 - P_b[\gamma(c_{i0}^r)]\}^L \quad (2.41)$$

where L is the frame length, $\gamma(c_{i0}^r)$ denotes the SINR at node r for bits transmitted by node i when none of node r's interferers transmits., and $P_b(\gamma)$ is the bit error rate for a certain SINR level γ.

2.5.3 Modelling the IEEE 802.11 DCF

In the backoff algorithm of IEEE 802.11 DCF, the states of channel can be classified in terms of three mutually exclusive events: E_c={collision}, E_i={idle channel}, and E_s={successful transmission}. To compute the channel state probabilities, the work by Bianchi [29] is utilized.

The average service time of every node in the network equals

$$\bar{T} = \bar{T}_B + \bar{T}_s \tag{2.42}$$

where $\bar{T}_B$ is the average back-off time, $\bar{T}_s$ is the average time for successful transmitting a packet at the end of the back-off operation.

Assume the Ad-Hoc network is saturate, and the average back-off time provided in [29] is given by

$$\overline{T_B} = \frac{\alpha(W_{min}\beta - 1)}{2q} + \frac{(1-q)}{q} t_c \tag{2.43}$$

where

$$\beta = \frac{q - 2^m(1-q)^{m+1}}{1-2(1-q)} \tag{2.44}$$

Parameter m represents the standard-definition maximum power utilized to set up the maximum window size, i.e., $W_{max} = 2^m W_{min}$. And $\alpha = \sigma p_i + t_c p_c + t_s p_s$, where $\boldsymbol{p_i}$=$[p_i^{\,i}$ $p_c^{\,i}$ $p_s^{\,i}]^T$ is the channel state probabilities vector for three events which node *i* can perceive during its back-off operation. And σ, t_c, t_s are the average times which correspond to each event respectively.

Probability vector $\boldsymbol{p_i}$ can be derived from the procedure below.

The probability that at any given time there are some nodes in node *i*'s sensing range transmitting a frame when node *i* is in back-off operation is,

$$p_{tr}^i = 1 - \prod_{j \in \mathrm{V_i}} (1 - \tau_j) \tag{2.45}$$

And the probability p_{suc}^i that a transmission within node *i*'s sensing range is successful is conditioned on the fact that at least one node in node i's sensing range attempts to transmit, i.e.,

$$p_{suc}^i = \frac{\sum_{k \in \mathrm{V_i}} P\{k\ transmits \cap \mathrm{k\ is\ successful}\}}{p_{tr}^i}$$

$$= \frac{\sum_{k\in \mathrm{V_i}} P\{\mathrm{k\ is\ successful} \mid k\ transmits\} P\{k\ transmits\}}{p_{tr}^{i}}$$

$$= \frac{\sum_{k\in \mathrm{V_i}} q_k \tau_k}{p_{tr}^{i}} \tag{2.46}$$

Therefore, the probability of a successful transmission occurs within node *i*'s sensing range, p_s^i is then $p_s^i = p_{tr}^i p_{suc}^i$. And the probability of idle channel within node *i*'s sensing range is then $p_i^i = 1\text{-}p_{tr}^i$, and the probability p_c^i which a collision happens within node *i*'s sensing range is given by $p_c^i = p_{tr}^i(1 - p_{suc}^i)$ [30]. After this channel state probabilities vector is determined, the average backoff time can be identified from equation (2.43) and the average service time can be derived from equation (2.42).

2.6 Simulation and Performance Evaluation

In this section, the simulations focus on the performance of the wireless Ad-Hoc networks with HSDPA system implemented on every wireless link. The first simulation is done to test and analyse the theoretical maximum achievable data rates of the one-group loading scheme and the two-group resource allocation scheme.

In Figure 2.5, a number of different transmission mechanisms are tested along with the two-group resource allocation scheme to inspect the theoretical overall achievable data rate in bits per symbol for a range of the received SNR, $\mathrm{SNR_T}$. In this simulation, several parameter values are given as $b_p \in \{2,4,6\}$, β=2 and $\Gamma = 7.8\mathrm{dB}$. The general rate allocation method is provided as

$$\mathrm{r} = \begin{cases} 0, \mathrm{if\ SNR_T} < \gamma(\mathrm{b_1}) \\ \mathrm{r(b_p)}, \mathrm{if}\ \gamma(\mathrm{b_p}) \le \mathrm{SNR_T} \le \gamma(\mathrm{b_{p+1}})\ \mathrm{for\ p} = 1,2 \\ \mathrm{r(b_3)}, \mathrm{if\ SNR_T} \ge \gamma(\mathrm{b_3}) \end{cases}$$

The single-code CDMA has only one channel to transmit data bit, and the required SNR for the single-code CDMA is $\gamma = \Gamma(2^{b_p} - 1)$, where $\mathrm{b_p}$ is the achievable data rate per symbol. The data rate per symbol achieved by this scheme is much lower than the data rates of the other two schemes.

The equal energy loading scheme and two-group resource allocation scheme are tested in HSDPA system with *K*=15 sub-channels. According to equation (2.5) (2.6), the data rate of one-group loading scheme is computed and plotted in Figure 2.5. It is clear that the data rate of this scheme is much higher than the achievable data rate of the single-code CDMA scheme.

The achievable data rate of the two-group resource allocation scheme is plotted as red line in Figure 2.5. As observed in this figure, the total data rate of the two-group resource allocation scheme is the highest in these three transmission mechanisms. It is because the residual transmission energy, which introduced in section 2.3.2, is well utilized by two-group resource allocation scheme. It should be noted that the reason for the total achievable data rates of one-group loading scheme and the two-group resource allocation scheme are equal to each other at last is the maximum b_p is b_3=6. When the SNR is very large, the maximum achievable data rate of two-group resource allocation scheme is limited to $r = Kb_3 = 15 \times 6 = 90$ bits per symbol. It means 15 sub-channels are fully loaded with the same bits per symbol $b_3 = 6$ which is equal to the single-group loading scheme.

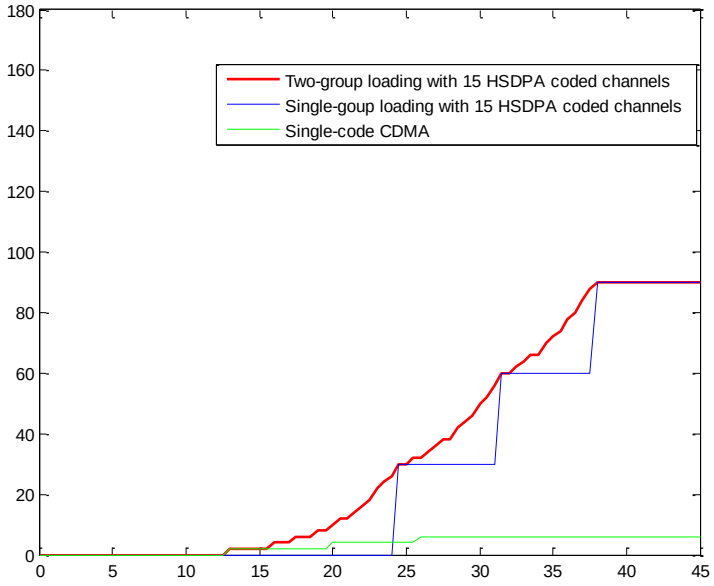

Figure 2.5 The data rate realized by different resource allocation schemes

However, in reality, the propagation distances in communication systems are relatively long which always leads to multipaths and frequency selective channels. Therefore, the second simulation is run to take the multipath effects into consideration. Consider two nodes in a wireless Ad-Hoc network, the maximum transmission range is 200 meters. The one-group loading scheme and the two-group resource allocation scheme are simulated with different propagation distance from 10 meters to 200 meters between two nodes. In this simulation model, the values of the parameters are set as $b_p \in \{2,4,6\}$, β=2 and $\Gamma = 7.8$dB. And a spreading matrix with number of sub-channels, K=15 and processing gain, N_{PG}=16 are

generated. The propagation loss is derived by using the two-ray ground reflection propagation model from equation (1.2). According to [13], the chiprate is set to 3.84Mbits/s, the transmission power at the source node is adjusted to 10 mW, and the power of noise is $P_{noise} = -93dBm$. And the additive white Gaussian noise of variance is given as

$$N_0 = P_{noise} T_c \tag{2.47}$$

where T_c represents the chip period. The overall available energy can be derived from

$$E_T = N_{PG} T_c P_T \tag{2.48}$$

And the resultant total received signal-to-noise ratio is

$$SNR_{Total} = \frac{10^{-h/10} E_T}{N_0} \tag{2.49}$$

where *h* denotes the propagation loss in dB.

The results are plotted in Figure 2.6 and 2.7.

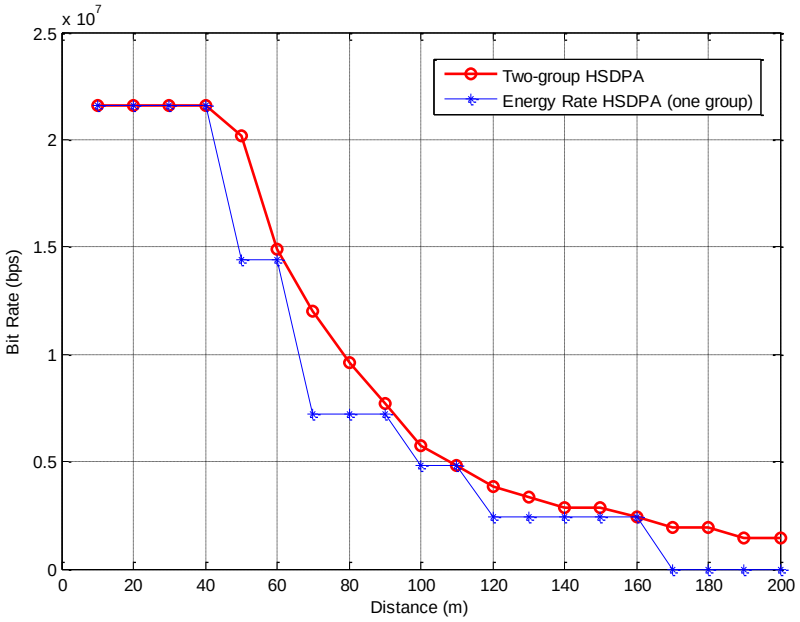

Figure 2.6 System capacity and bit rate achieved by One-group HSDPA system and Two-group HSDPA system as a function of distance

From Figure 2.6, it is observed that when the distance increases, the total achievable data rates of both one-group loading scheme and two-group resource allocation scheme decrease. It is because the propagation loss increases when the distance increases which leads to a reduction in the received signal power and the received SNR. And according to Figure 2.6, two-group resource allocation scheme has a larger total data rate than one-group loading scheme when the propagation distance exceeds 40 meters. And when the propagation

distance is larger than around 170 meters, the one-group loading scheme cannot support data transmission while the two-group resource allocation scheme still can achieve a total bit rate around 2 Mbits/s. It is because the one-group loading scheme can only use K=5, 10, 15 channels for transmission, however the two-group resource allocation scheme adopts a channel adaptive HSDPA system. The bit rates in Figure 2.6 are plotted along the received SNR in Figure 2.7. It is clear that due to its better residual energy utilization, the two-group resource allocation scheme has a larger bit rate than one-group loading scheme at certain SNR.

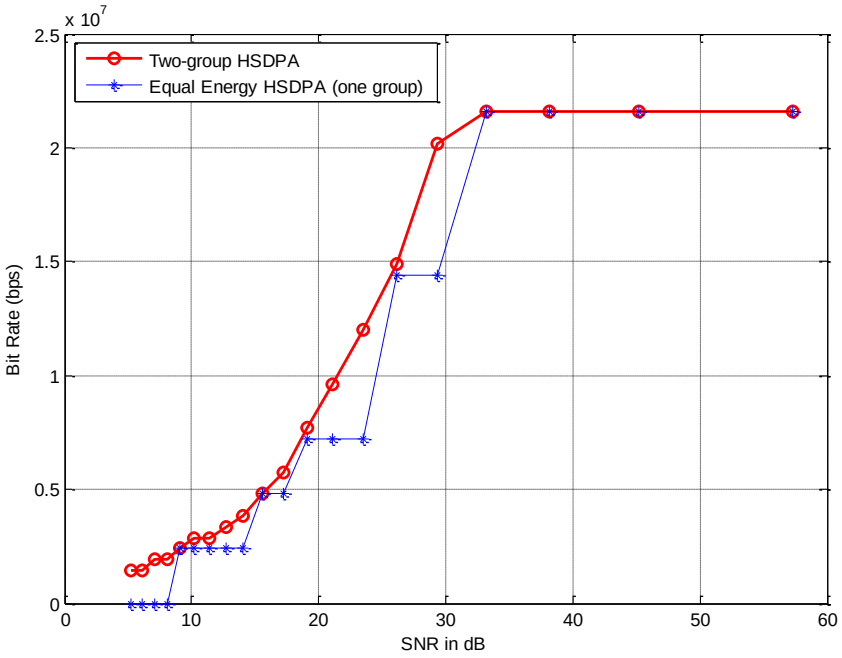

Figure 2.7 System capacity and bit rate achieved by One-group HSDPA system and Two-group HSDPA system as a function of SNR

Based on the DCF service time presented in this chapter, the final simulation has run to estimate and measure the end-to-end delay in a wireless Ad-Hoc networks. In Figure 2.8, a wireless Ad-Hoc network with 50 randomly distributed nodes is presented on an x-ygrid. And nodes in this networ are assumed stable with their ID marked besides them. The maximum transmission range of each node is set at 200 meter which indicates the signal can be detected at the received within this range. The maxmimum carrier sensing range at the MAC layer, which is defined as the range that the transmission power can be perceived, is given as 400 meters. And the nodes which can communicate with each other are linked with blue dash lines in Figure 2.8.

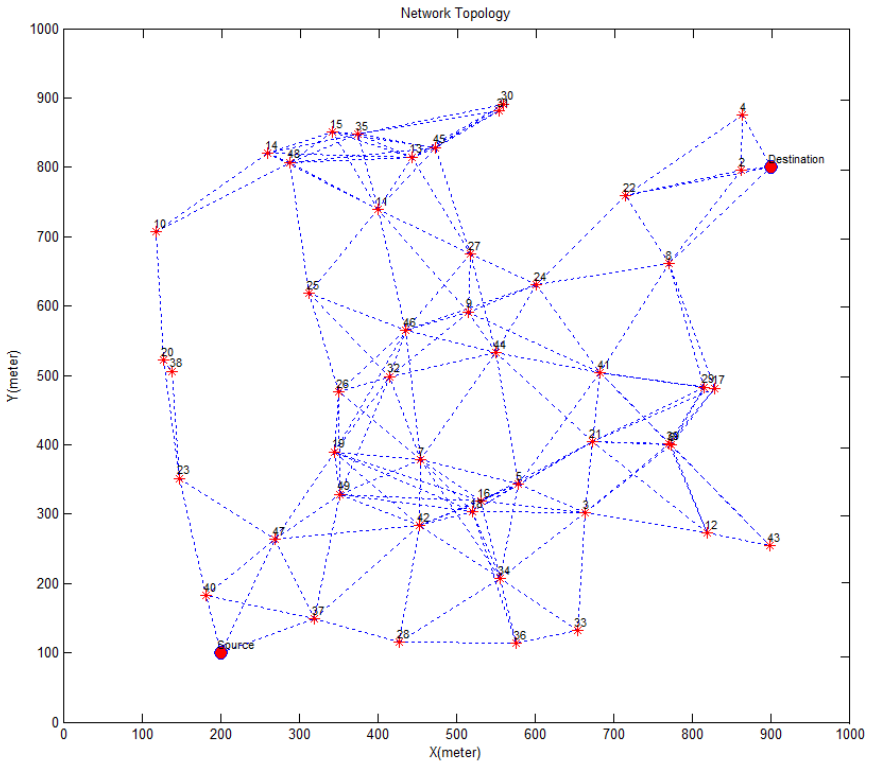

Figure 2.8 Network Topology

After the disjoint multiple paths from the source node and the destination node are discovered and constructed, the average service time of each node along the path can be identified from equation (2.4.2) and Carvalho model [19]. And then the maximum average service time of path z can be derived to choose the appropriate packet size L_z for path z. The end-to-end delay T_D^z indecates the time used in transmitting m_z bits from the source node to the destination node in packets of size L_z along path z. For a given time of T seconds and overall m_z bits to be transmitted in T seconds, the end-to-end delay is expected to be larger than T and can be estimated from

$$T_D^z = \left(\left\lfloor \frac{m_z}{L_z} \right\rfloor - 1\right) \max_{i,l \in Jz} \bar{T}_{i,l} + \sum_{i,l \in Jz} \bar{T}_{i,l} \qquad (2.50)$$

where $\bar{T}_{i,l}$ represents the average service time long the path z. the second term in equation (2.50) is the time used by the first packet transmitting from the source node to the destination node. And the first term indicates the time for transmitting the remaining packets.

Assume the paths with the least transmission energy consumption per bit from the source node to the destination node in a saturate wireless Ad-Hoc network can be found by disjoint

multipath routing discovery schemes. The disjoint multiple paths are shown in Firgure 2.9. The indexes of the nodes along two paths are given as

The best path: 1→40→47→49→19→26→32→46→9→24→22→2→50

The second best path: 1→37→42→18→16→5→21→41→8→50

Both one-group loading scheme and two-group rresource allocation scheme are implemented to assign achieveable data rate for each path.

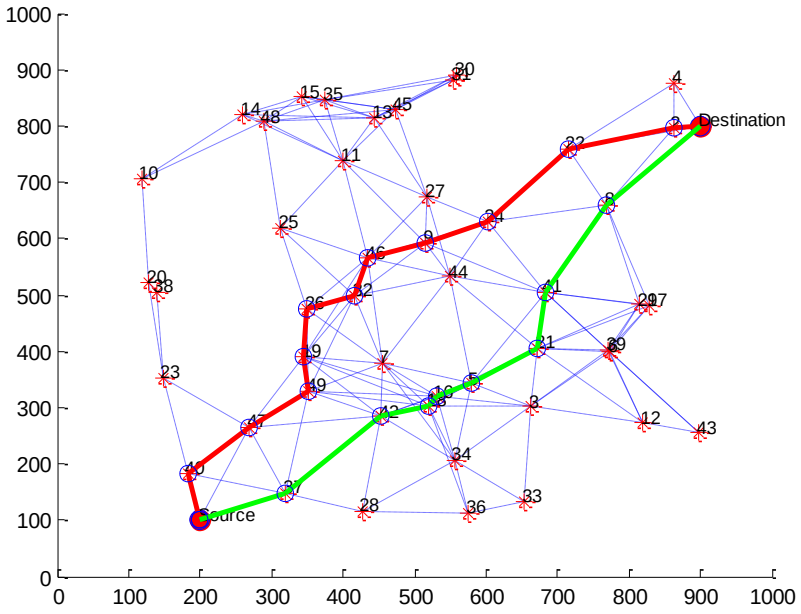

Figure 2.9 Network Topology with Disjoint Multiple Routing Paths

After the total data bit m_z for each path is allocated, the appropriate packet size is determined as

$$L_z = \frac{m_z}{T} \max_{i,l \in Jz} \bar{T}_{i,l} \tag{2.51}$$

And the number of packet can be derived from

$$N_z = \left\lfloor \frac{m_z}{L_z} \right\rfloor \tag{2.52}$$

As sometimes there are some remaining bits in m_z after N_z times of packet transmission, the packet size is then updated as

$$L_z = \left\lceil \frac{m_z}{N_z} \right\rceil \tag{2.53}$$

to ensure that all m_z bits are transmitted. In this simulation, the number of the total data bits is given as 1Mbits, and the target time of transmitting these bits is set at 20 s. The estimation end-to-end delay of twodifferent tranmission schemes are tested and illustrate in Figure 2.9. The maximum average service time for the paths adopting tow-group resource allocation scheme are 0.1692 s and 0.07845 s respectively. And the maximum average service time for one-group loading scheme are 0.1869 s and 0.07915 s respectively. From the Figure 2.10, we can observe that the end-to-end delay times are in the range between 20.5 seconds and 22.5 seconds. And the two-group loading scheme has a shorter end-to-end delay as expectation. It is because that in the same situation, the two-group resource allocation scheme can achieve a larger data bit rate than signle-group loading scheme. And due to less hops in the sencond path, the end-to-end delay time of the second path is less than the delay time in the first path.

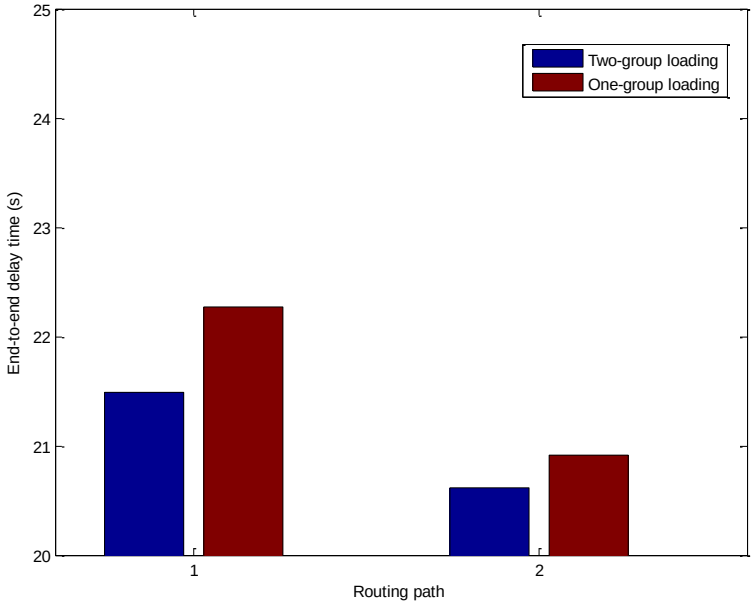

Figure 2.10 End-to-end delay predicted from equation (2.50)

Chapter 3

Disjoint Multipath Routing Discovery Schemes

3.1 Introduction

Unlike the traditional cellular communication systems in which the communications between the mobile nodes and administration infrastructure are direct without relays, the wireless Ad-Hoc networks do not have a centralized point for administration. The transmission and receiving between the source and the destination are realized by forwarding information from one node to another through a routing path. And the relay nodes consume some extra energy. Moreover, each node in these networks operates on constrained battery power, which eventually gets exhausted with time, thus energy is one of the most important constraints to be considered. To transmit more information in a certain lifetime, the routing path discovery schemes which consider the energy constraint should be developed.

3.2 Minimization of Energy Consumption Per Bit

A saturated wireless Ad-Hoc network is considered in this project with N randomly distributed nodes on a two-dimension grid. The maximum achievable data rate between each wireless link depends on the propagation distance between the transmitter and the receiver which causes a different amount of SNR for data transmission. For this reason, different wireless routes may have various numbers of bits per symbol to transmission. And different packet sizes are adjusted and adopted in different routing paths according to the computed energy consumption per bit for the path.

Consider a source node and destination node in a network, a total number of M bits to be transmitted over Z routing paths linking from the source to the destination in T seconds. The total transmission data rate between the source and the destination is provided as

$$R = \frac{M}{T}\ (bits/s) \tag{3.1}$$

Regarding path *z*, m_z bits of information are transmitted over this path at a rate of m_z/T bits per second for a given *T* seconds, where the total number of bits *M* is the sum of the bits transmitted in all the routing path exist which is defined as $M = \sum_{z=1}^{Z} m_z$. And $\overline{T_{i,j}}$ is the service time, which is defined and identified in Chapter 3, between node *i* and node *j*. Node *i* and node *j* are the adjacent nodes along the routing path. L_z is the packet size in bit transmitted over path *z*. Based on the parameters given above, the maximum transmission data rate over path *z* is given by

$$R_{z,max} = \frac{L_z}{\max(\overline{T_{i,j}})_{\mathrm{i,j}\in \mathrm{J_z}}} = \frac{m_z}{T} \tag{3.2}$$

where J_z represents the set of nodes in path *z*. And the total transmission data rate can be expressed as

$$R = \frac{M}{T} = \sum_{z=1}^{Z} \frac{m_z}{T} = \sum_{z=1}^{Z} \frac{L_z}{\max(\overline{T_{i,j}})_{\mathrm{i,j}\in \mathrm{J_z}}} \tag{3.3}$$

The amount of energy consumed to transmit m_z bits at a data rate of m_z/T bits per second over path *z* is given by

$$\begin{aligned} E_z &= m_z E_T \sum_{i,j\in J_z} \frac{1}{r_{i,j}} \\ &= m_z P_T N_{PG} T_c \sum_{i,j\in J_z} \frac{1}{r_{i,j}} \\ &= m_z E_{b,z} \end{aligned} \tag{3.4}$$

which requires an equivalent MAC power of $P_{MAC,z} = E_z/T$ and amount of energy consumed per bit over path z is

$$E_{b,z} = P_T N_{PG} T_c \sum_{i,j\in J_z} \frac{1}{r_{i,j}} \tag{3.5}$$

Thus, when the energy consumption for every routing path is known, the total consumed energy is proposed to be minimized as

$$\min(E_T) = \min(\sum_{z=1}^{Z} m_z E_{b,z}) \tag{3.6}$$

In order to minimize the total energy E_T, the least consumed amounts of energy per bit, $E_{b,z}$ must be determined as equation above. To achieve the load balancing, the amount of energy which are allocated to each path are equal, such as $E_1, E_2, \dots, E_Z$. Once all possible routing paths without shared nodes are discovered by using the least amount of energy per bit $E_{b,z}$ as the path metrics, the number of bits which should be assigned to each path can be

derived. Given the total number of bits M to be transmitted, the expression of the energy consumed at each path is then given as follows.

$$M = \sum_{z=1}^{Z} m_z = \sum_{z=1}^{Z} \frac{E_z}{E_{b,z}} \tag{3.7}$$

$$E_z = \frac{M}{\sum_{z=1}^{Z} 1/E_{b,z}} \tag{3.8}$$

Equation (3.8) can be substituted in equation (3.4) to acquire the number of bits per path, and m_z is given by

$$m_z = \frac{M}{1+\sum_{j\neq z}^{Z} \frac{E_{b,z}}{E_{b,j}}} \tag{3.9}$$

Therefore, the minimum energy consumed for transmitting m_z bits over path z is determined. The routing path discovery schemes which consider energy constraint and use $E_{b,z}$ as the path metrics are presented in the following section.

3.3 The Trellis-hop Diagram Routing Discovery Scheme

Consider a wireless Ad-Hoc network with N nodes and a trellis-hop diagram can be adopted to determine all the possible routing paths. The diagram is organized by arranging $N \times N$ nodes in which the first arranging the N nodes are in a column and similar columns of nodes are repeatedly drawn up to $N-1$ times next to the first column. According to the links between nodes in the network topology, the routing paths are determined by drawing the links from the source node to its neighbouring nodes, which are denoted in the next column [21]. And the same process starts from the drawing the link to the adjacent neighbouring node to the destination node.

A simple example which shows the whole procedure of Trellis-hop Diagram Routing Discovery approach in a 5-node network is presented below. The topology of the network is illustrated in Figure 3.1, and the distance between every two nodes is labelled beside each link in red.

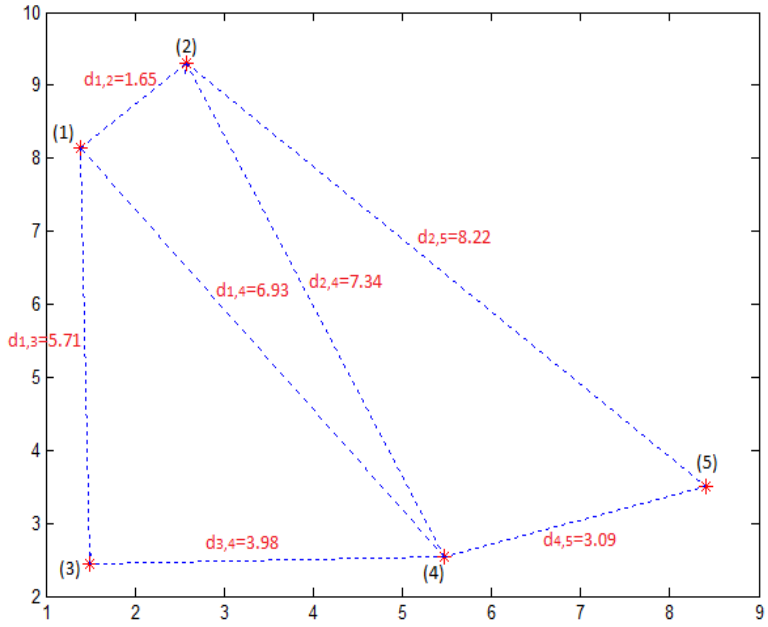

Figure 3.1 A 5-node Network Topology

From Figure 3.2-3.4, it is clear that two paths pass through neighbouring node 2 of the source node, two paths pass through source node's neighbouring node 3 and two paths pass through neighbouring node 4. Therefore, there are overall six paths from the source to the destination being determined by trellis-hop diagram. Then the energy consumed per bit for each path can be derived according to equation (3.5), and the one with the least energy consumption will be identified as the best path.

However, it is obvious that this approach has a significant extensive computational complexity. For the N-node Ad-Hoc network, this approach needs to compute *(N-1)!* times to find the path with the least cost, which is not efficient.

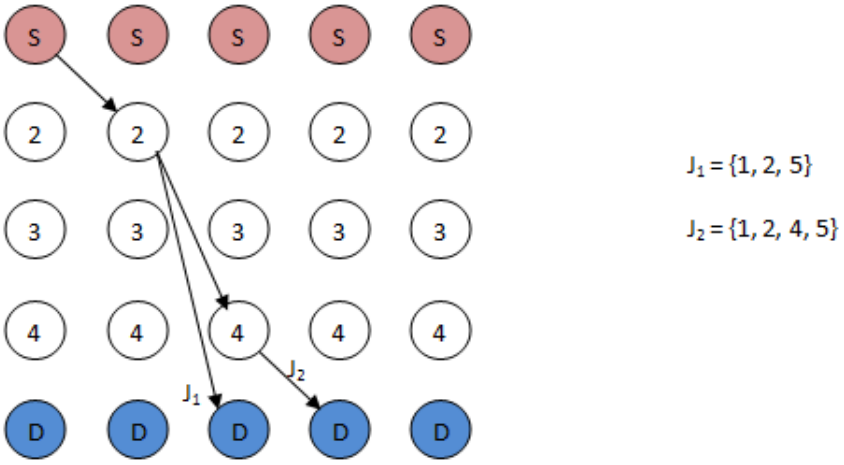

Figure 3.2 The First Neighbour of Source Node for Trellis-hop Diagram

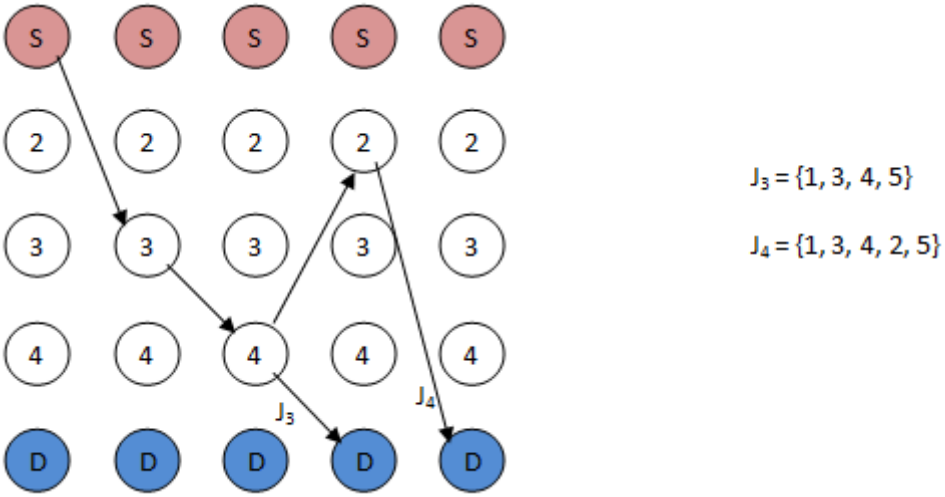

Figure 3.3 The Second Neighbour of Source Node for Trellis-hop Diagram

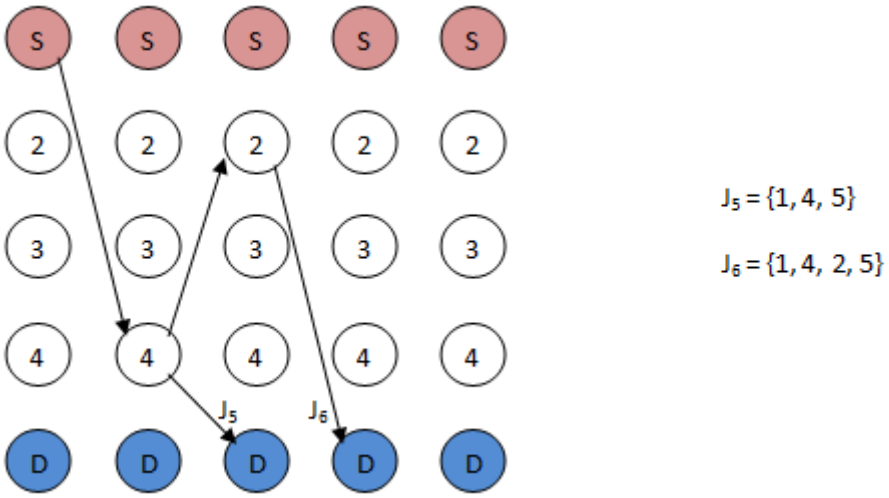

Figure 3.4 The Third Neighbour of Source Node for Trellis-hop Diagram

3.4 Modified Viterbi Algorithm

An improved version of Trellis-hop diagram approach which is named modified Viterbi algorithm is developed in [21] to improve the computational efficiency of Trellis-hop diagram approach. Instead of finding all the possible routes, this modified Viterbi algorithm groups the link-joint routing paths shared the same relay nodes and selects the routing path with the lowest cost as the best paths. The other high-cost paths are removed from the routing table during the routing path discovery process. Before commencing the routing path

discovery, the adjacency matrix is generated. The adjacency matrix for the topology in Figure 3.1 is given as

$$\mathbb{A} = \begin{bmatrix} 0 & 1 & 1 & 1 & 0 \\ 1 & 0 & 0 & 1 & 1 \\ 1 & 0 & 0 & 1 & 0 \\ 1 & 1 & 1 & 0 & 1 \\ 0 & 1 & 0 & 1 & 0 \end{bmatrix}$$

The entry of one in the adjacency matrix indicates the two nodes, which are represented by the indices or the row and column numbers of the entry, can communicate with each other. After the adjacent matrix is constructed, the data rate matrix can be formed as below.

$$\mathbb{R} = \begin{bmatrix} 0 & r_{1,2} & r_{1,3} & r_{1,4} & 0 \\ r_{2,1} & 0 & 0 & r_{2,4} & r_{2,5} \\ r_{3,1} & 0 & 0 & r_{3,4} & 0 \\ r_{4,1} & r_{4,2} & r_{4,3} & 0 & r_{4,5} \\ 0 & r_{5,2} & 0 & r_{5,4} & 0 \end{bmatrix}$$

The difference between the data rate matrix and the adjacency matrix is that the entries which are equal to one in the adjacency matrix are replaced with the data rate between the corresponding adjacent nodes. As the transmission power allocated in all the nodes are equal, the data rate matrix is symmetric, where $r_{i,j} = r_{j,i}$. It means the data rates are equal in both directions of any two adjacent nodes. Once the propagation path loss is derived by using the propagation model mentioned in equation (1.2), the received energy can be determined. Then the two-group resource allocation scheme is adopted to maximize the transmission data rate between every two nodes. Finally, the modified Viterbi algorithm can perform on the rate matrix to find the optimum paths.

In modified Viterbi algorithm, besides updating the total path link cost for all the latest paths which are discovered at each hop, it investigates the next nodes which are adjacent to the current nodes as well. In this process, the next node of each path cannot be the node which is already included in this path before. And all the incomplete paths are recorded in the incomplete routing table. Once the next node of the routing path is the destination node, this routing path is set to a completed path and stored in the completed routing table. If there are more than one incomplete routing paths which pass through the same next node, the routing path with the largest data rate and least energy consumption will be selected for further investigation, while the other paths will be abandoned. These processes will be iterated until all the nodes are investigated in and the optimal routing paths are found. There are three main

routing path tables for this algorithm and these are: (1) the completed routing path table, (2) the incomplete routing path table, and (3) the abandoned routing path table.

Figure 3.5-3.8 illustrate how this proposed algorithm operates at each hop level. For simplification and easier understanding, the abandoned routing path table shown in each figure only contents the abandoned paths at each step. Firstly, the neighbouring nodes of the source node are reached in one hop. A group of uncompleted routing paths are generated in this step, ie. {1, 2},{1, 3} and {1, 4}. In the next step, the nodes within two-hop distance from the source node are searched. The link costs are calculated using equation (3.4), and the routing paths, which share the same destination nodes in this hop, with the least cost will be remained for next step process, while the other routing path will be abandoned. In this step, the discarded paths are represented by dash lines. And routing path {1, 2, 5} is stored in the completed routing table. Figure 3.8 shows the process of the forth step. In each step, the algorithm ensures the paths which have the least energy cost with the same destination node in this hop are remained, and the next nodes chosen for each current incomplete routing path are not included by this path before. After the algorithm is finished, the abandoned routing path table and the incomplete routing path table are clear. As shown in Figure. 3.8, the final completed routing paths based on current topology are {1, 2, 5}, and {1, 2, 3, 4, 5}. And one of these three paths, which has the least energy consumption, will be selected as the best path.

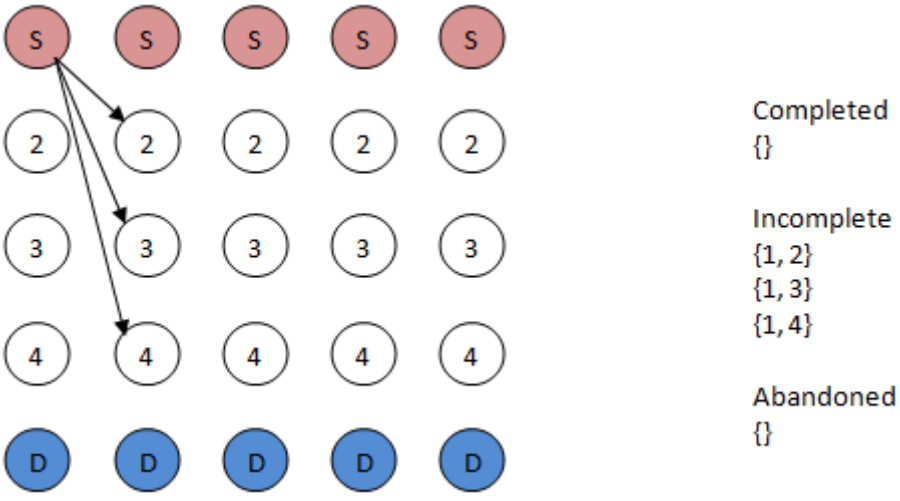

Figure 3.5 The First Hop Level for Routing Paths Discovery

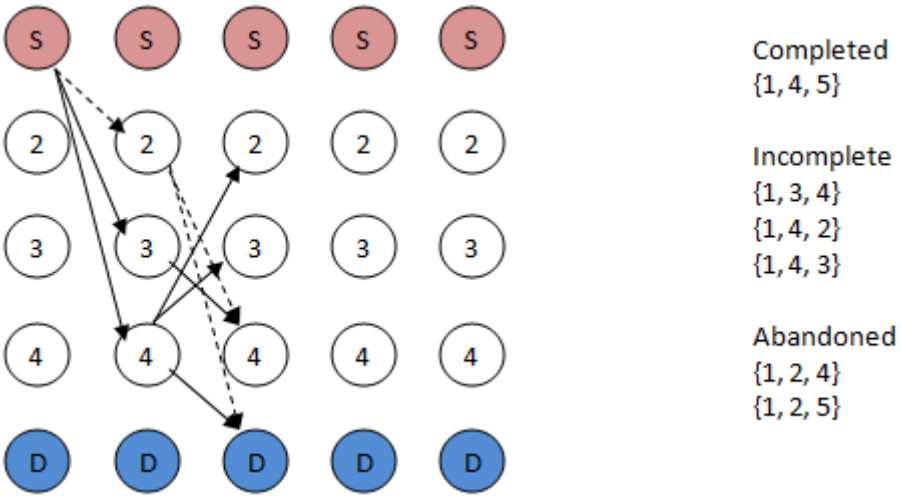

Figure 3.6 The Second Hop Level for Routing Paths Discovery

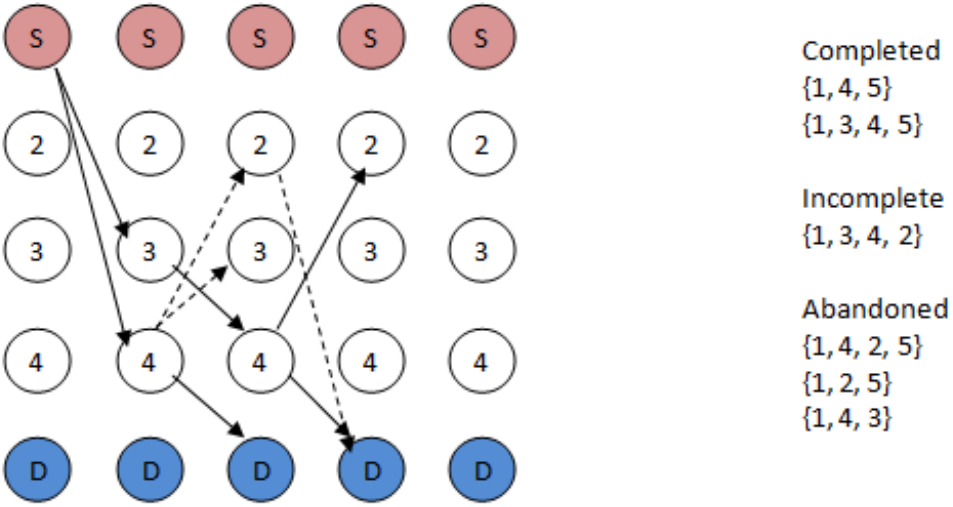

Figure 3.7 The Third Hop Level for Routing Paths Discovery

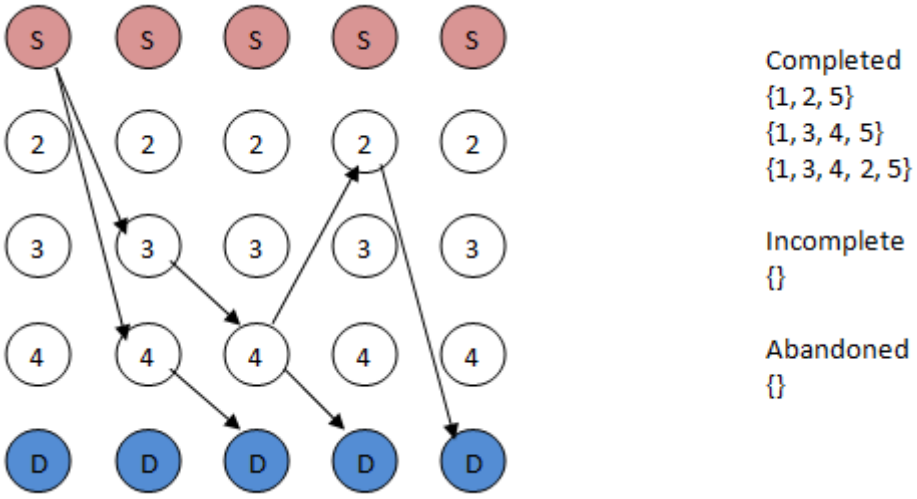

Figure 3.8 The Forth Hop Level for Routing Paths Discovery

It is obvious that as many incomplete paths with large link costs are not consider for further routing discovery in modified Viterbi algorithm, the modified Viterbi algorithm has a much better computational efficiency than trellis-hop diagram approach. The modified Viterbi algorithm can reduce the computational complexity down to O(N) for a *N*-node networks, when the maximum number of neighbouring nodes is much lower than *N* [31].

In order to find all the disjoint lowest cost routing paths, the paths with the lowest cost is first found and all the nodes along this path are removed from the network topology. Then the routing discovery scheme is re-invoked to find the second lowest cost path in the new network topology which is constructed by the rest of the nodes. This process iterates until all the disjoint routing paths are discovered.

3.5 Modified Floyd Algorithm

The modified Viterbi algorithm proposed in previous section is efficient to find the best path for one-pair node (one source and one destination) with a computational complexity of O(*N*). However, if this algorithm is adopted to find the shortest paths in a multi-source and multi-destination scenario, the computational complexity of finding all the vertex pairs will increase to O(N^3) in a *N*-node network. To further investigate and enhance the routing paths discovery algorithm, a modified Floyd algorithm is developed to minimize the computational complexity of finding the shortest paths for all-pair nodes in a wireless ad hoc network.

In Floyd's algorithm, a distance matrix is generated and utilized to discover the shortest paths between all-pair of nodes in a network [32]. Its main operation theory is concluded as follow. A distance weigh matrix $\boldsymbol{D}^{(0)}$ is first constructed in which the each element denotes the distance between two adjacent nodes. Then the one-hop distances between each pair of nodes are computed and compared with the corresponding elements in distance matrix $\boldsymbol{D}^{(0)}$. The smaller distances for each pair of nodes are updated and stored in matrix $\boldsymbol{D}^{(1)}$. This process operates iteratively, and the distance matrixes for various hops are derived as $\boldsymbol{D}^{(2)}$, $\boldsymbol{D}^{(3)}$, …, $\boldsymbol{D}^{(k-1)}$, $\boldsymbol{D}^{(k)}$. The whole operation stops until $\boldsymbol{D}^{(k)}=\boldsymbol{D}^{(k-1)}$ which means the elements in distance matrix cannot be reduced anymore. And the least distances between all-pair of nodes are stored in $\boldsymbol{D}^{(k)}$which becomes the shortest distance matrix. The Floyd's algorithm is summarized as follows.

Step 1: Initial distance matrix $\boldsymbol{D}^{(0)}=(d_{ij}^{(0)})$,

where $d_{ij}^{(0)} = \begin{cases} w_{ij}, \text{weight of edge}(distance) \\ 0, i = j \\ \infty, if\ there\ is\ no\ edge\ between\ i\ and\ j \end{cases}$

Step 2: Generate iterative distance matrix $\boldsymbol{D}^{(k)}=(d_{ij}^{(k)})$, where $d_{ij}^{(k)} = \min\left\{d_{ir}^{(k-1)} + d_{rj}^{(k-1)} \middle| r = 1,2,\dots,n\right\}$.

Step 3: If $\boldsymbol{D}^{(k+1)}=\boldsymbol{D}^{(k)}$, loop stops; otherwise repeat step 2.

According to [32], the time complexity of Floyd's algorithm is $O(N^3)$ which is very high and not efficient for large networks. To improve the computational complexity of both the Floyd's algorithm and data rate allocation along the routing paths, a modified Floyd's algorithm is developed in the thesis.

As same as the Modified Viterbi Algorithm presented previously, in order to maximize the data rate of the routing path under certain transmission energy, the two-group resource allocation scheme is applied to derive the maximum data rate between every pair of the adjacent nodes. In this process, the equation (1.2) is used to derive the propagation loss which affects the SNR and the received energy in every wireless link. From equation (2.2) (2.3) (2.10) (2.15), it is clear that the only external factor effects the data rate distribution is the distance between two nodes. When the distance (d) increases, the propagation loss increases proportionately to the quartic power of distance (d^4). And the received energy decreases when the propagation loss increases, which leads to a reduction in transmission data rate. Therefore, , in order to reduce the computational complexity, the quartic power of the distance between each two nodes ($d_{i,j}^4$) which are in each other's transmission range is adopted as the metric of a weigh matrix, instead of utilizing the maximum data rate between every pair of the adjacent nodes to construct a rate matrix in modified Viterbi algorithm. For instance, the weigh matrix of the topology in Figure 3.1 is given by

$$\mathbb{W}^{(0)} = \begin{bmatrix} 0 & w_{1,2} & w_{1,3} & w_{1,4} & \infty \\ w_{2,1} & 0 & \infty & w_{2,4} & w_{2,5} \\ w_{3,1} & \infty & 0 & w_{3,4} & \infty \\ w_{4,1} & w_{4,2} & w_{4,3} & 0 & w_{4,5} \\ \infty & w_{5,2} & \infty & w_{5,4} & 0 \end{bmatrix}$$

$$= \begin{bmatrix} 0 & d_{1,2}^4 & d_{1,3}^4 & d_{1,4}^4 & \infty \\ d_{2,1}^4 & 0 & \infty & d_{2,4}^4 & d_{2,5}^4 \\ d_{3,1}^4 & \infty & 0 & d_{3,4}^4 & \infty \\ d_{4,1}^4 & d_{4,2}^4 & d_{4,3}^4 & 0 & d_{4,5}^4 \\ \infty & d_{5,2}^4 & \infty & d_{5,4}^4 & 0 \end{bmatrix}.$$

The shortest path in this algorithm is the path has the least sum of the quartic power of all the hop distances along the routing path, which is defined as $min(\sum_{z=1}^{Z} d_{ij}^4)_{i,j\in J_z}$.And J_Z is the set of the nodes along the path.

After analyzing the basic Floyd's algorithm, four points are investigated in and modified to accelerate the calculation speed and reduce the computational complexity.

1) It is not difficult to find that when deriving the elements $w_{ij}^{(k)}$ of the weigh matrix $\boldsymbol{W}^{(k)}$, the elements $w_{st}^{(k)}$ (s=1,2,3…*i-1*; t=1,2,…n) in previous *i-1* rows, and the previous *j-1* elements $w_{it}^{(k)}$ (t=1,2,3…j-1) in i^{th} row have already been calculated. In this way, the Gauss Seidel algorithm [34] can be applied in these elements to derive the shortest path. As $w_{ij}^{(k)}=\min\{w_{ir}^{(k-1)}+w_{rj}^{(k-1)}|r=1,2,\ldots,n\}$, when $r<j$, we have $w_{ir}^{(k)}\leq w_{ir}^{(k-1)}$; when $r<i$, we have $w_{rj}^{(k)}\leq w_{rj}^{(k-1)}$. Thus it is possible to use $w_{ir}^{(k)}$ and $w_{rj}^{(k)}$ to replace $w_{ir}^{(k-1)}$ and $w_{rj}^{(k-1)}$. And the shortest path equation can be written as

$$w_{ij}^{(k)} = \min\{\min\{w_{ir,r<j}^{(k)}+w_{rj,r<i}^{(k)}\}, \min\{w_{ir,r<j}^{(k)}+w_{rj,r>j}^{(k-1)}\}, \min\{w_{ir,r>j}^{(k-1)}+w_{rj,r<i}^{(k)}\}, \min\{w_{ir,r>j}^{(k-1)}+w_{rj,r>i}^{(k-1)}\}\}. \quad (3.10)$$

2) In the Floyd's algorithm, backtrace is adopted to find the shortest path from the source to the destination. It means that in order to find the shortest path between node *i* and node *j*, the algorithm have to trace back to the previous steps to determine how $w_{ij}^{(k)}$ comes from. For example, let $w_{ij}^{(k)}= w_{ir}^{(k-1)}+ w_{rj}^{(k-1)}$. Then, the algorithm will check how $w_{ir}^{(k-1)}$ and $w_{rj}^{(k-1)}$ are determined. This process iterates until the elements in $\boldsymbol{W}^{(0)}$ are reached. To simplify this complicated approach, a routing matrix which records all the routing paths for different pairs of nodes is generated as $L^{(k)}=(l_{ij}^{(k)})$. For example, let $l_{ij}^{(k)}=\{ l_{ir}^{(k-1)}$, node r, $l_{rj}^{(k-1)}\}$, the elements in $l_{ij}^{(k)}$ denote the nodes which the path from node *i* to node *j* passes through. When the iteration ends and the routing matrix becomes to $\boldsymbol{L}^{(k)}$, the shortest path between node i and node j can be expressed as $i \rightarrow l_{ij}^{(k)} \rightarrow j$.

3) As in wireless Ad-Hoc network, the distance from node *i* to node *j* is equal to the distance from node *j* to node *i*, we have $d_{ij}^4=d_{ji}^4$ and $w_{ij}^{(k)}=w_{ji}^{(k)}$. In this way, if $w_{ij}^{(k)}$ has already been determined, it is not necessary to use more iterations to derive $w_{ji}^{(k)}$.

4) When derive the shortest path between two nodes *i* and *j*, the distances are compared first before adding together. For example, if $w_{ir}^{(k-1)} \geq w_{ij}^{(k-1)}$ or $w_{rj}^{(k-1)} \geq w_{ij}^{(k-1)}$, it is clear that the distance between node *i* and node *j* will increase if nodes *r* is inserted, thus it is not necessary to derive $w_{ir}^{(k-1)}+w_{rj}^{(k-1)}$.

Therefore, the process of the modified Floyd's algorithm can be presented as follows:

Step 1: Initialize a weigh matrix $\mathbf{W}^{(0)}=(w_{ij}^{(0)})$, in which

$$w_{ij}^{(0)} = \begin{cases} d_{ij}^4, \text{ when node i and node j are adjacent} \\ 0, when\ i = j \\ \infty, when\ node\ i\ and\ node\ j\ cannot\ communicate\ with\ each\ other \end{cases}$$

Initialize a routing matrix $\mathbf{L}^{(0)}=(l_{ij}^{(0)})$, where

$$l_{ij}^{(0)} = \begin{cases} \phi, \text{ when node i and node j are adjacent and i=j} \\ -, when\ node\ i\ and\ node\ j\ cannot\ communicate\ with\ each\ other \end{cases}$$

Step 2: Generate the iterative weigh matrix $\boldsymbol{W}^{(k)}$ and the routing matrix $\boldsymbol{L}^{(k)}$:

Each node *r* from node *1* to node *n* when *r≠i,j* are checked. If $w_{ir}^{(k-1)} \geq w_{ij}^{(k-1)}$ or $w_{rj}^{(k-1)} \geq w_{ij}^{(k-1)}$ which indicates the inserting of node *r* into the path between node *i* and node *j* cannot decrease the transmission energy consumption, therefore $w_{ir}^{(k-1)} + w_{rj}^{(k-1)}$ is not necessary to be computed. Otherwise, $w_{ij}^{(k)} = \min\{w_{ij}^{(k-1)}, w_{ir}^{(k-1)} + w_{rj}^{(k-1)}\}$ for the k-th iteration. The routing matrix will update with the weigh matrix correspondingly. If $w_{ij}^{(k)} < w_{ij}^{(k-1)}\ and\ w_{ij}^{(k)} = w_{ir}^{(k-1)} + w_{rj}^{(k-1)}$, the index of node r should be included in the corresponding element $l_{ij}^{(k)}$ in the routing matrix, which is give as

$$l_{ij}^{(k)} = \{l_{ir}^{(k-1)},\ r,\ l_{rj}^{(k-1)}\} \tag{3.11}$$

Otherwise, the corresponding element in the routing matrix will not change, $l_{ij}^{(k)} = l_{ij}^{(k-1)}$.

Step 3: If $\boldsymbol{W}^{(k+1)}=\boldsymbol{W}^{(k)}$, iteration stops, and the best paths of all pairs of nodes are recorded in the routing matrix; otherwise repeat step 2.

This modified Floyd's algorithm is also applied on the network with the topology shown in figure (3.1) to find the best paths between any two nodes. The initial weigh matrix and routing matrix can be acquired as follows.

$$\mathbb{W}^{(0)} = \begin{bmatrix} 0 & d_{1,2}^4 & d_{1,3}^4 & d_{1,4}^4 & \infty \\ d_{2,1}^4 & 0 & \infty & d_{2,4}^4 & d_{2,5}^4 \\ d_{3,1}^4 & \infty & 0 & d_{3,4}^4 & \infty \\ d_{4,1}^4 & d_{4,2}^4 & d_{4,3}^4 & 0 & d_{4,5}^4 \\ \infty & d_{5,2}^4 & \infty & d_{5,4}^4 & 0 \end{bmatrix}.$$

$$= \begin{bmatrix} 0 & 7.5 & 1062.0 & 2308.8 & \infty \\ 7.5 & 0 & \infty & 2910.9 & 4565.7 \\ 1062.0 & \infty & 0 & 251.1 & \infty \\ 2308.8 & 2910.9 & 251.1 & 0 & 90.8 \\ \infty & 4565.7 & \infty & 90.8 & 0 \end{bmatrix}$$

$$\mathbb{L}^{(0)} = \begin{bmatrix} \phi & \phi & \phi & \phi & - \\ \phi & \phi & - & \phi & \phi \\ \phi & - & \phi & \phi & - \\ \phi & \phi & \phi & \phi & \phi \\ - & \phi & - & \phi & \phi \end{bmatrix}$$

According to step 2, as $w_{11}^{(0)} = 0$, it is not necessary to calculate $w_{11}^{(1)}$. We have $w_{11}^{(1)} = w_{11}^{(0)} = 0$ and $l_{11}^{(1)} = l_{11}^{(0)} = \phi$ correspondingly.

$w_{12}^{(1)}$: as none of the elements in the first row of $W^{(0)}$ is smaller than $w_{12}^{(0)}$(except $w_{11}^{(0)}$), it is not necessary to calculate $w_{1r}^{(0)} + w_{r2}^{(0)}$. We have $w_{12}^{(1)} = w_{12}^{(0)}$, and in the routing matrix $l_{12}^{(1)} = l_{12}^{(0)} = \phi$.

$w_{13}^{(1)}$: as there is an element in the first row of $W^{(0)}$ which is smaller than $w_{13}^{(0)}$, $w_{13}^{(1)}$ is defined as $w_{13}^{(1)} = \min\{w_{13}^{(0)}, w_{12}^{(0)} + w_{23}^{(0)}\} = w_{13}^{(0)}$ =1062.0. The corresponding element in routing matrix remains the same, $l_{13}^{(1)} = l_{31}^{(0)} = \phi$. And $w_{13}^{(1)} = w_{31}^{(1)} = 1062.0$, $l_{31}^{(1)} = l_{13}^{(1)} = \phi$.

$w_{14}^{(1)}$: as there are two elements in the first row of $W^{(0)}$ are smaller than $w_{14}^{(0)}$, $w_{14}^{(1)}$ is defined as $w_{14}^{(1)} = \min\left\{w_{14}^{(0)}, w_{12}^{(0)} + w_{24}^{(0)}, w_{13}^{(0)} + w_{34}^{(0)}\right\} = w_{13}^{(0)} + w_{34}^{(0)} = 1313.1$, which means node 3 is inserted into the path between node 1 and node 4. And $l_{14}^{(1)} = \{3\}$. Moreover, $w_{41}^{(1)} = w_{14}^{(1)} = 1313.1$, $l_{41}^{(1)} = l_{14}^{(1)} = \{3\}$.

Similarly, the other elements in $W^{(1)}$ and $L^{(1)}$ can be determined.

$w_{15}^{(1)} = \min\left\{w_{15}^{(0)}, w_{12}^{(0)} + w_{25}^{(0)}, w_{14}^{(0)} + w_{45}^{(0)}\right\} = w_{14}^{(0)} + w_{45}^{(0)} = 2399.6$, $l_{15}^{(1)} = \{3, 4\}$.

$w_{51}^{(1)} = w_{15}^{(1)} = 2399.6$, $l_{51}^{(1)}$=$l_{15}^{(1)} = \{3, 4\}$

$w_{21}^{(1)} = w_{21}^{(0)}$, $l_{21}^{(1)} = \phi$.

$w_{22}^{(1)} = w_{22}^{(0)} = 0$, $l_{22}^{(1)} = l_{22}^{(0)} = \phi$.

$w_{23}^{(1)} = \min\left\{w_{23}^{(0)}, w_{21}^{(1)} + w_{13}^{(1)}\right\} = w_{21}^{(1)} + w_{13}^{(1)} = 1069.5$, $l_{23}^{(1)} = \{1\}$.

$w_{32}^{(1)} = w_{23}^{(1)} = 1069.5$, $l_{32}^{(1)} = l_{23}^{(1)} = \{1\}$.

$w_{24}^{(1)} = \min\left\{w_{24}^{(0)}, w_{21}^{(1)} + w_{14}^{(1)}, w_{23}^{(1)} + w_{34}^{(0)}\right\} = w_{21}^{(1)} + w_{14}^{(1)} = w_{23}^{(1)} + w_{34}^{(0)} = 1320.6$,

$l_{24}^{(1)} = \left\{l_{21}^{(1)}, 1, l_{14}^{(1)}\right\} = \left\{l_{23}^{(1)}, 3, l_{34}^{(0)}\right\} = \{1, 3\}$.

$w_{42}^{(1)} = w_{24}^{(1)} = 1320.6$, $l_{42}^{(1)} = l_{24}^{(1)} = \{1,3\}$.

$w_{25}^{(1)} = \min\left\{w_{25}^{(0)}, w_{21}^{(1)} + w_{15}^{(1)}, w_{23}^{(1)} + w_{35}^{(0)}, w_{24}^{(1)} + w_{45}^{(0)}\right\} = w_{24}^{(1)} + w_{45}^{(0)} = 1411.4$,

$l_{25}^{(1)} = \left\{l_{24}^{(1)}, 4, l_{45}^{(1)}\right\} = \{1,3,4\}$.

$w_{52}^{(1)} = w_{25}^{(1)} = 1411.4$, $l_{52}^{(1)} = l_{25}^{(1)} = \{1, 3, 4\}$.

$w_{33}^{(1)} = w_{33}^{(0)} = 0$, $l_{33}^{(1)} = l_{33}^{(0)} = \phi$.

$w_{34}^{(1)} = w_{34}^{(0)} = 251.1$, $l_{34}^{(1)} = l_{34}^{(0)} = \phi$.

$w_{43}^{(1)} = w_{34}^{(1)} = 251.1$, $l_{43}^{(1)} = l_{34}^{(1)} = \phi$.

$w_{35}^{(1)} = \min\left\{w_{35}^{(0)}, w_{31}^{(1)} + w_{15}^{(1)}, w_{32}^{(1)} + w_{25}^{(1)}, w_{34}^{(1)} + w_{45}^{(0)}\right\} = w_{34}^{(1)} + w_{45}^{(0)} = 341.9$, $l_{35}^{(1)} = \left\{l_{34}^{(1)}, 4, l_{45}^{(0)}\right\} = \{4\}$.

$w_{44}^{(1)} = w_{44}^{(0)} = 0$, $l_{44}^{(1)} = l_{44}^{(0)} = \phi$.

$w_{45}^{(1)} = w_{45}^{(0)} = 90.8$, $l_{45}^{(1)} = l_{45}^{(0)} = \phi$.

$w_{54}^{(1)} = w_{45}^{(1)} = 90.8$, $l_{54}^{(1)} = l_{45}^{(1)} = \phi$.

$w_{55}^{(1)} = w_{55}^{(1)} = 0$, $l_{55}^{(1)} = l_{55}^{(0)} = \phi$.

After the derivation above, we have

$$\mathbb{W}^{(1)} = \begin{bmatrix} 0 & 7.5 & 1062.0 & 1313.1 & 2399.6 \\ 7.5 & 0 & 1069.5 & 1320.6 & 1411.4 \\ 1062.0 & 1069.5 & 0 & 251.1 & 341.9 \\ 1313.1 & 1320.6 & 251.1 & 0 & 90.8 \\ 2399.6 & 1411.4 & 341.9 & 90.8 & 0 \end{bmatrix}$$

$$\mathbb{L}^{(1)} = \begin{bmatrix} \phi & \phi & \phi & 3 & 3,4 \\ \phi & \phi & 1 & 1,3 & 1,3,4 \\ \phi & 1 & \phi & \phi & 4 \\ 3 & 1,3 & \phi & \phi & \phi \\ 3,4 & 1,3,4 & 4 & \phi & \phi \end{bmatrix}$$

As $W^{(1)} \neq W^{(0)}$, the iteration should be carried out until $W^{(k)} \neq W^{(k-1)}$. $W^{(2)}$ and $L^{(2)}$ are obtained as follows.

$$\mathbb{W}^{(2)} = \begin{bmatrix} 0 & 7.5 & 1062.0 & 1313.1 & 2399.6 \\ 7.5 & 0 & 1069.5 & 1320.6 & 1411.4 \\ 1062.0 & 1069.5 & 0 & 251.1 & 341.9 \\ 1313.1 & 1320.6 & 251.1 & 0 & 90.8 \\ 2399.6 & 1411.4 & 341.9 & 90.8 & 0 \end{bmatrix}$$

$$\mathbb{L}^{(2)} = \begin{bmatrix} \phi & \phi & \phi & 3 & 3,4 \\ \phi & \phi & 1 & 1,3 & 1,3,4 \\ \phi & 1 & \phi & \phi & 4 \\ 3 & 1,3 & \phi & \phi & \phi \\ 3,4 & 1,3,4 & 4 & \phi & \phi \end{bmatrix}$$

It is clear that $\boldsymbol{W}^{(2)} = \boldsymbol{W}^{(1)}$, and the algorithm terminates. Therefore, the best paths of every two nodes in the network are recorded in the routing matrix. For example, according to the routing matrix, the best path between node 1 and node 5 passes through node 3 and node 4.

After the best path is found between the source node and the destination node, two-group resource allocation scheme will then adopted to determine the maximum data rate for each single hop along the best path. Obviously, instead of determining the data rate between every two nodes in the network, this algorithm reduces the computational complexity greatly. In Figure 3.9, the modified Viterbi algorithm and modified Floyd's algorithm are adopted to find the disjoint multiple routing paths.

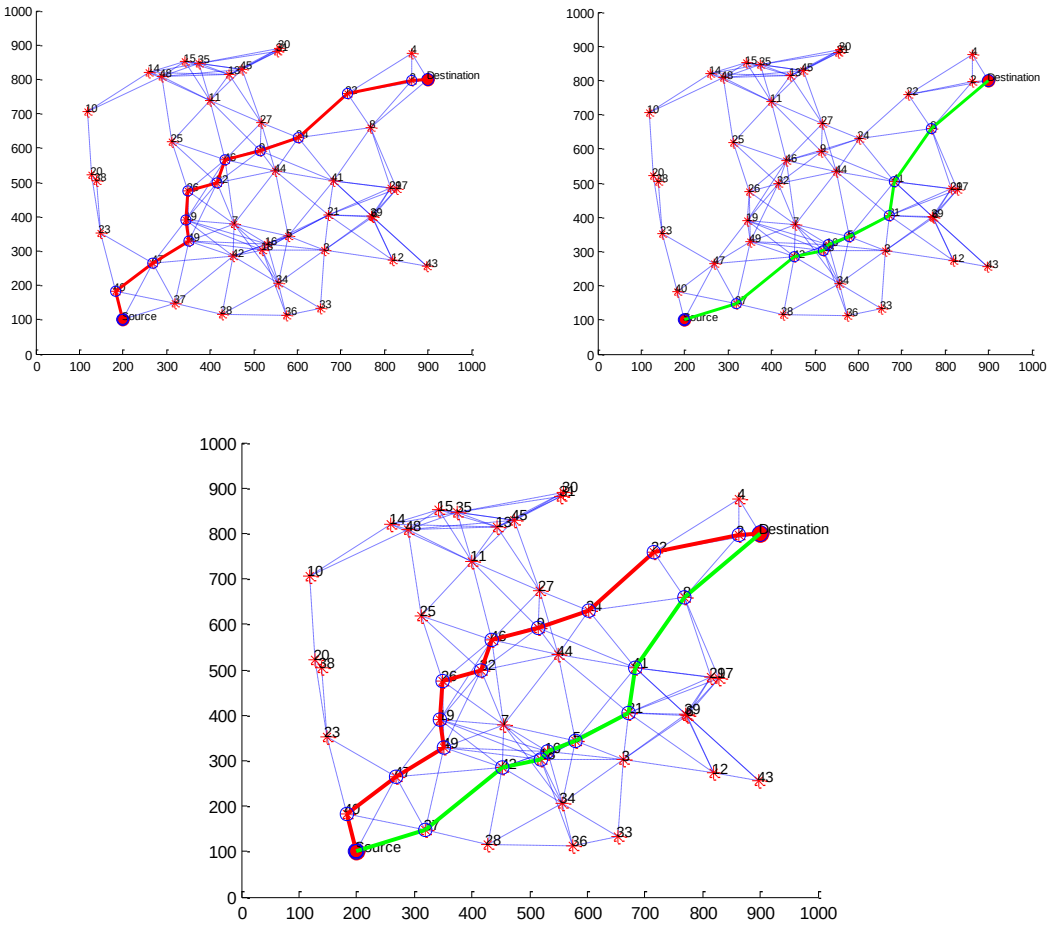

Figure 3.9 Disjoint Multiple Routing Discoveries

3.6 Performance Evaluation

As mention in section 3.4, the computational complexity for trellis-hop diagram routing method is O(N^3). And the modified Viterbi algorithm can enhance the efficiency significantly and reduce the computational complexity to O(N). On the other hand, the computational complexity of the modified Viterbi algorithm in finding the all-pair best paths is O(N^3). In order to order to efficiently find the best paths between every two nodes in a network, the modified Floyd's algorithm is developed to enhance the efficiency of the traditional Floyd's algorithm. Compared with the traditional Floyd's algorithm, the number of iterations is reduced in the modified algorithm. As the comparisons of $\left(w_{ij}^{(k-1)}, w_{ir}^{(k-1)}\right) and\ (w_{ij}^{(k-1)}, w_{rj}^{(k-1)})$ are done before deriving $w_{ij}^{(k)}$, $w_{ir}^{(k-1)} + w_{rj}^{(k-1)}$ is not necessary to be calculated at each iteration. Thus, the computational complexity is less than O(N^3). Moreover, after the analysis, it is not difficult to find that at k-iteration to

derive $w_{ij}^{(k)}$, the nodes with $w_{ir}^{(k-1)} = \infty$, which cannot communicate with the node *i*, will not be considered. Therefore, it just needs to consider m_i nodes which can communicate with node i. Let m_i be the number of edges connected with node i. As there are N^2 elements in the weigh matrix, it needs m_i times operation to derive w_{ij}^{k} and the computational complexity at *k*-iteration is $\sum_1^{N^2} m_i$. And $w_{ij}^{(k-1)}$ is equal to $w_{ji}^{(k-1)}$ in this case, when $w_{ij}^{(k-1)}$ is derived, $w_{ji}^{(k-1)}$ is known as well. Therefore, the computational complexity of this modified Floyd's algorithm is $O(\frac{m}{2} \cdot N^2)$ which is less than the computational complexity of the traditional Floyd's algorithm.

Chapter 4

Coded Parity Packet Scheme

4.1 Introduction

In telecommunication systems, retransmissions are carried out to achieve the reliable packet transmission when data packets fail to be detected at the receiver end. In wireless Ad-Hoc networks, unnecessary repetitive retransmissions cause not only an increase in the end-to-end delay, but also a rise in the energy consumption of nodes, which would reduce the network lifetime significantly when the nodes are battery powered. Increasing the transmission energy per symbol can increase the output SNR and reduce the number of retransmissions. However, as this approach consumes a great amount of additional energy, the network lifetime would be significant reduced. Therefore, the packet error rate should be minimized by lowering the increase in the required energy close to the theoretical minimum value [35]. It is essential to develop a channel coding scheme to reduce the gap value in wireless Ad-Hoc networks, which keeps the packet error rate low and decreases the number of retransmissions whilst providing lower energy consumption. Hence, the Coded Parity Packet Approach [22] is developed by M. K. Gurcan to lower the packet error rate and then reduce the retransmission times and the required energy. Coded Parity Packet Approach includes an outer and inner coding scheme to provide alternative additional information value for the decoding process. Without changing the effective code rate, the outer coding technique adjusts the number of source and parity packets, from which the additional input information values are produced on the receiver end to be alternatively fed into the decoding process to recover the received packets.

4.2 System Overview

It is considered that the system is constructed by three main blocks, such as the transmitter, the channel and the receiver, as shown in Figure 4.1. The discrete information from the data

source is in binary form. The data sequences are generated in blocks of K symbols, and each block is denoted as a $(K \times 1)$-dimensional vector $\bar{u}$, in which each of its element is represented as $u_k \in \{\pm 1\}$, for $k = 1,2,...,K$.

The source data block is segmented into V equal-sized source packets, and each of them represented as an $((N\text{-}N_p) \times 1)$ - dimensional vector, $\overline{u_v}$, where $N\text{-}N_p=K/V$. And then the outer coder will use these source packets to produce $E\text{-}V$ parity packets in addition to the V source packets which are denoted as $\overline{s_e}$. After this, N_p cyclic redundancy check (CRC) bits are appended to each parity packets which yields $(N \times 1)$ – dimensional vector $\overline{C_e}$. At last, these packets are inner coded to create $(B \times 1)$-dimensional vector $\overline{x_e}$ for e=1, 2…, E. before transmission in wireless channel, a modulated symbol vector $\overline{y_e}$ is produced from every coded packet $\overline{x_e}$ by adopting an M-QAM scheme. The generated symbols are transmitted over a noise-corrupted channel, in which the white Gaussian noise vector is denoted by $\overline{n_e}$ with a variance of $\sigma^2 = N_0$.

At the receiver end, after the noise-corrupted symbols $\overline{w_e} = \overline{y_e} + \overline{n_e}$ are demodulated, the required $(B \times 1)$-dimensional soft channel output vector $\Lambda(\overline{x_e})$, which is the input of the iterative soft decoding process, is derived from the received symbol vector $\overline{w_e}$ [23]. Then, the CRC-appended packets $\overline{c_e}$ is estimated by the soft-in-hard-out decoding process at the receiver. The CRC algorithm is re-invoked to check the integrity of these estimates [36]. Each CRC-checked vector is represented as $\widehat{\overline{s_e}}$. Before the final estimates are de-segmented, if any of the first V parity packets $\widehat{\overline{s_1}}$, $\widehat{\overline{s_2}}$, …, $\widehat{\overline{s}}_V$, which are the source packets $\widehat{\overline{u_1}}$… $\widehat{\overline{s_V}}$, fail then a hard decoding mechanism will operate to recover these packets.

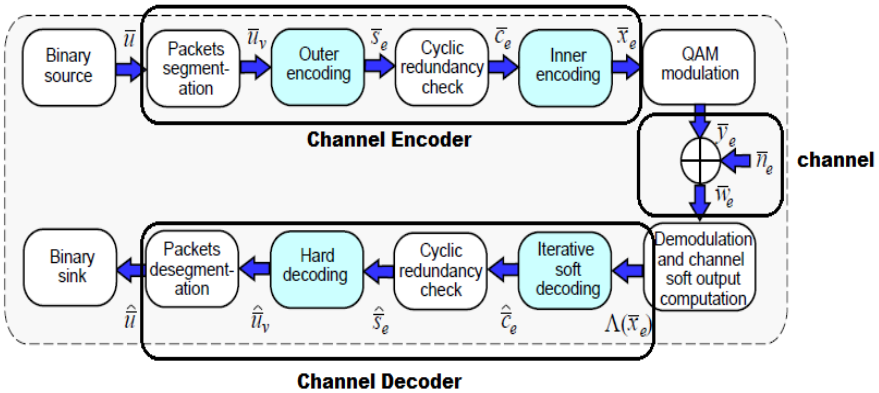

Figure 4.1 The Coded Parity Packets Approach Model

4.3 Channel Encoder

The channel encoder can be separated to twp parts – outer encoder and inner encoder.

4.3.1 The Outer Encoder

The data block after packets segmentation can be represented in a matrix as **U** = [$\overline{u_1}$, $\overline{u_2}$, …, $\overline{u_V}$]. These source packets are passed through the outer encoder to produce *E* packets, **S** = [$\overline{s_1}$,…, $\overline{s_E}$]. There are *E*-*V* parity packets in these *E* packets. The formula to generate these E packets can be expressed as below.

$$\boldsymbol{S} = \boldsymbol{U} \otimes \boldsymbol{G} \tag{4.1}$$

As there are *E*-*V* parity packets, L_E=$2^{E\text{-}V\text{-}1}$ subsets of associated packets are generated. If the outer code rate is fixed at $r_{out} = \frac{V_0}{E_0}$, the number of the subsets, L_E can be controlled by adjusting the integer numbers V_0 and E_0 of the source and parity packets to $V = V_0 \times \alpha$ and $E = E_0 \times \alpha$ such that the outer code rate $r_{out} = \frac{V_0}{E_0} = \frac{V}{E}$ remains unchanged, where α is the adjustment parameter [23].

α	The number of subsets, L_E				
	$E_o - V_o = 1$	$E_o - V_o = 2$	$E_o - V_o = 3$	…	$E_o - V_o > 0$
1	1	2	4	…	$2^{E_o - V_o - 1}$
2	2	8	32	…	$2^{2(E_o - V_o) - 1}$
3	4	32	256	…	$2^{3(E_o - V_o) - 1}$
⋮	⋮	⋮	⋮	…	⋮
α	$2^{\alpha - 1}$	$2^{2\alpha - 1}$	$2^{3\alpha - 1}$	…	$2^{\alpha(E_o - V_o) - 1} = 2^{E - V - 1}$

Table above shows that the number of distinct subsets of the parity packets, L_E, is controllable, therefore it can be increased to enhance both the soft and hard decoding process on the receiver end.

The matrix **G** in equation (4.1) can be generated from

$$\boldsymbol{G} = [\boldsymbol{I}_V \; \boldsymbol{P}\boldsymbol{J}^{(sel)}] \tag{4.2}$$

where $\boldsymbol{I}_V$ is a (*V*×*V*)-dimensional identity matrix which is used to regenerate the *V* source packets. And $\boldsymbol{P}\boldsymbol{J}^{(sel)}$ is the generator for *E*-*V* parity packets. $\boldsymbol{P}$ is a (*V*×*Z*)-dimensional matrix, while $\boldsymbol{J}^{(sel)}$ is a *(Z×(E-V))*-dimensional parity selector matrix. Each column in matrix $\boldsymbol{P}$ can be derived by

$$\overline{p_z} = \boldsymbol{J}_V bin(D) \tag{4.3}$$

where bin(*D*) represents a (*V*×*1*)-dimensional binary vector which corresponds to a number *D*. *D* can be treat as the index which points from 3 to 2^V-1 so long as *D* is not a power of two. $\boldsymbol{J}_V$ is a (*V*×*V*)-dimensional matrix which has its cross diagonal elements equal to 1 and other elements equal to 0.

To ensure that the parity selector matrix, $\boldsymbol{J}^{(sel)}$,selects E source and parity packets from which $2^{E\text{-}V\text{-}1}$ subsets of parity packets are available to generate $2^{E\text{-}V\text{-}1}$ subsets, every source packet must be a neighbour of at least one of the parity packets [23]. The simplest way to make every source packet as a neighbour of at least one parity packet is making this parity packet be generated from the last column $\overline{p_z}$ in matrix P, because $\overline{p_z}$=[1,1,1,…,1]^T. The remaining *E-V-1* parity packets can be produced by using the remaining columns in P. Thus, $\boldsymbol{PJ}^{(\text{sel})}$ in equation (4.2) can be written as

$$\begin{aligned} \mathbf{PJ}^{(sel)} &= \begin{bmatrix} p_{Z-(E-V-1),1} & & 0 & 1 \\ p_{Z-(E-V-1),2} & & 1 & 1 \\ \vdots & \cdots & \vdots & \vdots \\ p_{Z-(E-V-1),V} & & 1 & 1 \end{bmatrix} \\ &= \left[\overline{p}_{Z-(E-V-1)}, \cdots, \overline{p}_{Z-1}, \overline{p}_Z\right]. \end{aligned} \tag{4.4}$$

where $\bar{p}_{Z-(E-V-1)} = [p_{Z-(E-V-1),1}, p_{Z-(E-V-1),2}, \dots, p_{Z-(E-V-1),V}]^T$. Therefore, $\boldsymbol{J}^{(\text{sel})}$ can be written as follows

$$\mathbf{J}^{(sel)} = \begin{bmatrix} \mathbf{0}_{(Z-(E-V))\times(E-V)} \\ \mathbf{I}_{E-V} \end{bmatrix} \tag{4.5}$$

According to the $\boldsymbol{J}^{(\text{sel})}$ generated above, the parity packets $\bar{s}_e$ can be derived from equation (4.1) and (4.2).

4.3.2 The Inner Encoder

The inner encoders are the standard Turbo encoders with an inner code rate of r_{in}= *N/B*. The CRC-appended parity packets, $\bar{c}_e$ produced by the outer encoder are sent to the inner encoders. Then a M-QAM modulation scheme operates on these coded parity packets. A modulated packet, $\bar{y}_e = [y_{e,1}, \dots, y_{e,j}, \dots, y_{e,J}]^T$ is Gray-mapped from a Turbo-coded parity packet which is represented as a *(B×1)*-dimensional vector $\bar{x}_e = [\bar{x}_{e,1}^T, \dots, \bar{x}_{e,j}^T, \dots, \bar{x}_{e,J}^T]^T$. And the vectors in $\bar{x}_e$ can be expressed as $\bar{x}_{e,j} = [x_{e,j,1}, \dots, x_{e,j,m_i}, \dots, x_{e,j,m}]^T$. As Turbo codes are adopted as the inner codes, which are generated from the parity packets, there are three categories of the coded parity bits. The first category is the systematic bit, $x_{e,n}^{(n)} = x_{e,n}$; the

second category is the first parity bit, $x_{e,n_{p1}}^{(p1)}$; the third category is the second parity bit, $x_{e,n_{p2}}^{(p2)}$ These three types of bits depend on the puncturing performed on the Turbo codes for $n=1,\ldots,N$, $n_{p1}=1,\ldots,N_{p1}$, $n_{p2}=1,\ldots,N_{p2}$, where $N + Np1 + Np2 = B$.

4.4 Channel Decoder

In this section, the decoding process of Coded Parity Packet approach is described.

The received packet is given by $\overline{w_e} = [w_{e,1}, \ldots, w_{e,j}, \ldots, w_{e,J}]^T$, and the corresponding channel soft output, as the source of input soft information for soft decoding, is defined as $\Lambda(x_{e,j,m_i})$ which is given by

$$\Lambda\left(x_{e,j,m_i}\right) = \frac{1}{N_0}\left(min_{\varsigma_0 \in S_{mi}^0} ||w_{e,j} - \varsigma_0||^2 - min_{\varsigma_1 \in S_{mi}^1} ||w_{e,j} - \varsigma_1||^2\right). \tag{4.6}$$

Unlike [37] which makes an assumption that the channel gain is unity, S_{mi}^0 and S_{mi}^1 are two sets of symbols which denote the sets of symbols in which the m_i-th component of $(m\times1)$-vector, $\overline{x_{e,j}}$, ie. $x_{e,j,mi}$, equal to 0 and 1 respectively. Hence, the members in set S_{mi}^0 and S_{mi}^1 are represented by ς_0 and ς_1 respectively.

At the receiver side, E standard Turbo decoders are working in parallel, and each of them has two component decoders. The channel soft outputs of each packet are demultiplexed into two sequences. The first sequence which includes the LLRs of the systematic bits, $\Lambda(x_{e,n}^{(s)})$ and the first set of parity bits, $\Lambda(x_{e,n}^{(p1)})$ for n = 1, . . . , N and e = 1, . . . , E is fed into the first component decoder. And the second sequence, which comprises the LLRs of the systematic bits, $\Lambda(x_{e,n}^{(s)})$ and the second set of parity bits, $\Lambda(x_{e,n}^{(p2)})$, is fed into the second component decoder. The LLRs for the parity bits are produced according to the Turbo code rate adopted, $r_{in}= N/B$. The channel soft outputs provided from the systematic bits, $\Lambda(x_{e,n}^{(s)})$, are defined as the *apriori* LLRs.

$$\Lambda_{apri}\left(x_{e,n}^{(1)}\right) = \Lambda_{ext}\left(x_{e,n}^{(2)}\right) + \Lambda\left(x_{e,n}^{(s)}\right) + \Lambda_{ext}^{E}\left(x_{e,n}\right), \tag{4.7}$$

$$\Lambda_{apri}\left(x_{e,n}^{(2)}\right) = \Lambda_{ext}\left(x_{e,n}^{(1)}\right) + \Lambda\left(x_{e,n}^{(s)}\right) + \Lambda_{ext}^{E}\left(x_{e,n}\right). \tag{4.8}$$

where $\Lambda_{apri}\left(x_{e,n}^{(1)}\right)$ and $\Lambda_{apri}\left(x_{e,n}^{(2)}\right)$ represent the *apriori* LLRs of the first component decoder and second component decoder respectively. The *extrinsic* LLR, Λ_{ext}, and the *external extrinsic* LLR, Λ_{ext}^{E}, which are generated from the previous iteration, are zero in the

first iteration. If the *apriori* LLRs are added up with more reliable soft information, the chance of correctly decoding will increase. Another two types of LLRs are generated, after the *apriori* LLRs are generated and passed into the component decoders in each iteration. The first and second component decoders produce

- *aposterior* LLRs, $\Lambda_{apos}\left(x_{e,n}^{(1)}\right)$ and $\Lambda_{apos}\left(x_{e,n}^{(2)}\right)$, and
- *extrinsic* LLRs, $\Lambda_{ext}\left(x_{e,n}^{(1)}\right)$ and $\Lambda_{ext}\left(x_{e,n}^{(2)}\right)$.

The *aposterior* LLRs can be derived from a modified log-MAP algorithm [37] which is given by

$$\Lambda_{apos}\left(x_{e,n}^{(1)}\right) = \log\left(\frac{P\left(x_{e,n}=+1|\Lambda\left(x_{e,n}^{(p1)}\right),\Lambda_{apri}\left(x_{e,n}^{(1)}\right)\right)}{P\left(x_{e,n}=-1|\Lambda\left(x_{e,n}^{(p1)}\right),\Lambda_{apri}\left(x_{e,n}^{(1)}\right)\right)}\right) \tag{4.9}$$

$$\Lambda_{apos}\left(x_{e,n}^{(2)}\right) = \log\left(\frac{P\left(x_{e,n}=+1|\Lambda\left(x_{e,n}^{(p2)}\right),\Lambda_{apri}\left(x_{e,n}^{(2)}\right)\right)}{P\left(x_{e,n}=-1|\Lambda\left(x_{e,n}^{(p2)}\right),\Lambda_{apri}\left(x_{e,n}^{(2)}\right)\right)}\right) \tag{4.10}$$

The *aposteriori* LLRs are then adopted to generate the *extrinsic* LLRs,

$$\Lambda_{ext}\left(x_{e,n}^{(1)}\right) = \Lambda_{apos}\left(x_{e,n}^{(1)}\right) - \Lambda_{apri}\left(x_{e,n}^{(1)}\right), \tag{4.11}$$

$$\Lambda_{ext}\left(x_{e,n}^{(2)}\right) = \Lambda_{apos}\left(x_{e,n}^{(2)}\right) - \Lambda_{apri}\left(x_{e,n}^{(2)}\right). \tag{4.12}$$

$\Lambda_{ext}\left(x_{e,n}^{(1)}\right)$ and $\Lambda_{ext}\left(x_{e,n}^{(2)}\right)$ are exchanged between two component decoders after the first iteration finished. And when the number of decoding iterations in the component decoders reaches the maximum number, the $\Lambda_{ext}\left(x_{e,n}^{(2)}\right)$ in the second component decoder is taken to generate the *extrinsic* LLR, where $\Lambda_{ext}(c_{e,n}) = \Lambda_{ext}\left(x_{e,n}^{(2)}\right)$ corresponds to packet $\bar{c}_e$. The ($N \times E$) dimensional extrinsic LLR matrix, $\mathbf{\Lambda}_{ext}$, which is formed by the *extrinsic* LLR vectors, can be written as follows

$$\mathbf{\Lambda}_{ext} = [\Lambda_{ext}(\bar{c}_1), \dots, \Lambda_{ext}(\bar{c}_e), \dots, \Lambda_{ext}(\bar{c}_E)]. \tag{4.13}$$

where $\Lambda_{ext}(\bar{c}_e)$ represents the *extrinsic* LLR column vector with elements of $\Lambda_{ext}\left(c_{e,n}\right)$ for n=*1,…,N*.

There are $L_E=2^{E-V-1}$subsets of *extrinsic* LLRs, which can generate *extrinsic* LLRs, for each of *E* received packets. In order to identify these subsets, a matrix which is called

extended parity check decoding matrix, is adopted. The extended parity check decoding matrix, which is a ($E\times(2^{(E-V)}-1)$)-dimensional matrix, can be derived from

$$\boldsymbol{H} = \boldsymbol{H}_{base} \otimes [\boldsymbol{I}_{(E-V)}\ \boldsymbol{Y}] \tag{4.14}$$

where $\mathbf{H}_{\text{base}} = \begin{bmatrix} \mathbf{PJ}^{(sel)} \\ \mathbf{I}_{E-V} \end{bmatrix}$. When $(E-V)>1$, Y is a $((E-V)\times(2^{(E-V)}-(E-V)-1))$-dimensional matrix with columns $\bar{y}_f$ for f=$1,\ldots, 2^{(E-V)}-(E-V)-1$ which is obtained from $\bar{y}_f = \mathbf{J}\text{bin}(F)$ [23]. bin(F) is just as same as the bin(D) in encoding process, where F=3,…, $(2^{(E-V)}-1)$. When $(E-V)$=1, **Y** is a null matrix, because there is only one column of H is required to represent the single set of accompany parity packet, in which $\boldsymbol{I}_{(E-V)}$ equals to one.

After the process above, $2^{(E-V)}$-1 columns of matrix $\boldsymbol{H} = [\bar{h}_1,..,\bar{h}_{2^{(E-V)}-1}]$ can be generated And with this extended parity check decoding matrix, the subsets of the *extrinsic* LLRs can be configured, as for each received parity packet being decoded, an *extrinsic* LLR is generated. Since the columns in matrix H denotes a unique subset of associated parity packets for a given V and E. For each source packet, $\bar{c}_e$ has L_e associated *external extrinsic* LLR matrices, $\boldsymbol{A}_{ext}^{(e,l)}$. L_e represents the overall number of ones along row e of matrix **H**. This associated *external extrinsic* LLR matrix, $\boldsymbol{A}_{ext}^{(e,l)}$ is generated from

$$\boldsymbol{A}_{ext}^{(e,l)} = \boldsymbol{\Lambda}_{ext}\boldsymbol{J}_{e,l}^{(sel)} \quad \text{for } l = 1,\ldots,L_e \tag{4.15}$$

where $\boldsymbol{J}_{e,l}^{(sel)}$ is the $(E\times N_{s,e,l})$-dimensional parity selector matrix with column vectors, $\bar{J}_{e,l,i}$ obtaining all the elements equal to zero except an unity element at the column number which is corresponding to the column number of the element with *i-th* unity value in vector $\bar{h}_{e,l}$. The associated set vector, $\bar{h}_{e,l}$ is the column vector of **H** which corresponds to the *l-th* associated *external extrinsic* LLR matrices $\boldsymbol{\Lambda}_{ext}$of the source packet $\bar{c}_e$. And $N_{s,e,l}$ is the number of ones in vector $\bar{h}_{e,l}$. The process of the *external extrinsic* LLR generation is illustrated in Figure 4.2.

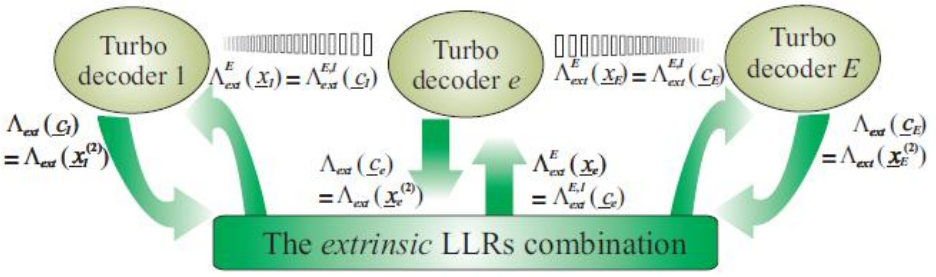

Figure 4.2 The process of the external extrinsic LLR generation [23]

According to the definition presented above, the associated *external extrinsic* LLR matrix, $\boldsymbol{A}_{ext}^{(e,l)}$ can be expressed as

$$\boldsymbol{A}_{ext}^{(e,l)} = [\bar{a}_{ext,1}^{(e,l)}, \dots \bar{a}_{ext,i}^{(e,l)}, \dots, \bar{a}_{ext,N_{s,e,l}}^{(e,l)}]. \tag{4.16}$$

The simplified *extrinsic* LLRs combination function mentioned in [38] is given by

$$[\Lambda_{ext}^{E,l}(\bar{c}_e)]_n = \min_i |[\bar{a}_{ext,i}^{(e,l)}]_n| \prod_{i=1}^{N_{s,e,l}} sign([\bar{a}_{ext,i}^{(e,l)}]_n), \tag{4.17}$$

where $[\Lambda_{ext}^{E,l}(\bar{c}_e)]_n$ and $[\bar{a}_{ext,i}^{(e,l)}]_n$ represent the elements of *external extrinsic* LLR vector and the *extrinsic* LLR vector respectively for n=1,…,N. this simplified calculation is iterate for n=1,…,N to acquire the LLR vector $\Lambda_{ext}^{E,l}(\bar{c}_e)$which is then obtained as the *external extrinsic* LLR vector at the *l-th* iteration, $\Lambda_{ext}^{E}(\bar{x}_e) = \Lambda_{ext}^{E,l}(\bar{c}_e)$. Therefore, at any single external iteration, only a single *external extrinsic* LLR vector is produced. The external iteration will terminate once the maximum iteration number is reached or the packet is successfully decoded. After obtaining $\Lambda_{ext}^{E}(x_{e,n})$, $\Lambda(x_{e,n}^{(s)})$, $\Lambda_{ext}\left(x_{e,n}^{(1)}\right)$ and $\Lambda_{ext}\left(x_{e,n}^{(2)}\right)$, the *apriori* LLRs, which are derived from the equation (4.7) (4.8), are enhanced to continue the decoding process.

If the received packets are not successfully decoded in the iterative soft decoding process which presented above, a packet-based hard decoding approach is adopted to solve this problem. After all the successfully decoded packets are hard decided from the soft bits provided by the iterative soft decoding process and denoted as $\hat{\bar{c}}_e$ for e=1,…,E, the integrity of these packets are checked by the CRC algorithm. And $\hat{\bar{s}}_e$ are used to represents the output packets. To successfully hard decode a received packet, the equation below should be satisfied.

$$\boldsymbol{I}_c \times \bar{h}_{e,l} = \bar{h}_{e,l} \text{ for } l = 1, \dots, L_E \tag{4.18}$$

where $\bar{h}_{e,l}$ is introduced in the iterative soft decoding process, and $\boldsymbol{I}_c$ is a (E×E)-dimensional diagonal matrix which is defined as

$$\boldsymbol{I}_c = diag(\bar{h}_c), \tag{4.19}$$

The diagonal components are the elements, $h_{c,e}$ of vector $\bar{h}_c$, are all zero except for those with the indices equal to the indices of the successfully decoded packet. For example when E=5, $\bar{h}_c = [1\ 0\ 0\ 1\ 1]^T$ indicates that the first, the forth and the fifth received packets are soft decoded successfully.

If the equation (4.18) is satisfied, the e-th packet can be recovered as follows.

$$\hat{\tilde{s}}_e = \bar{h}_{e,l}^T \otimes \mathbf{I}_c \hat{\mathbf{S}}^T \tag{4.20}$$

where $\hat{\mathbf{S}}^T$ is a (E×N)-dimensional matrix in which the rows are produced after the iterative soft decoding process, $\hat{\mathbf{S}}^T = [\hat{\tilde{s}}_1, \dots, \hat{\tilde{s}}_E]^T$.

Obviously, the performance of the hard decoding process is enhanced as more selections for bit-wise XOR combinations between packets are available to recover the failed packets. Therefore, when α increases and $L_E = 2^{\alpha(E_0 - V_0)-1}$ increases, the packet error rate will be reduced.

4.5 Performance Analysis of CPP Approach in Wireless Ad-Hoc Networks

In this section, transmission scheme and re-transmission schemes are first explained and analysed for the point-to-point transmission. Then an adjustable transmission protocol for wireless Ad-Hoc network is developed and presented.

Consider the wireless transmission on a single hop between two nodes in a wireless Ad-Hoc network. It is assumed that the location of each node is stable. The transmission energy can be written as $E_p = nE_b$, where *n* denotes the number of bits, and E_b represents the energy required to transmit one single bit. E_b is influenced by the distance between two nodes and the resource allocation scheme.

The packet error rate, p_p, measures the probability of a packet is detected error at the receiver. This probability mainly depends on the network protocols and the packet size. And many uncontrollable and unpredictable factors can influence it as well. The bit error rate, p_e is assumed to be independent on different bits. And the data packet error rate without re-transmission for a packet with *k* bits is given by

$$p_p = 1 - (1 - p_e)^k \tag{4.21}$$

A re-transmission is usually requested to reduce the packet error rate when the data packet is detected erroneous at the receiver. It is assumed the errors in the received packets can be detected at the receiver end. The packet error rate after α times re-transmission can be reduced to

$$p'_p = {p_p}^{\alpha+1} \quad for\ \alpha = 0,1,\dots N \tag{4.22}$$

It is clear that when the bit error rate is fixed at a certain value, the packet error rate increases when the packet size increases. However, some other bits are contented in every packet besides the information bits, such as the packet header. Therefore, though the packet error rate can be reduced by adopting a smaller packet size, a larger overhead in term of transmission energy and bandwidth is raised due to less information data in each packet. Detained studies on the trade-off between the packet size and the overhead are analysed in [39].

4.5.1 Basic Retransmission Schemes

Three re-transmission schemes in wireless communication systems are considered and presented below. For notational convenience, several mathematical notations are presented here. Let k bits in one packet. p_e denotes the bit error rate. p_p represents the packet error rate without re-transmission. And E_b is the energy per bit.

Case I: Time Sensitive Re-transmission

If errors are detected in the received packet, a re-transmission request will be sent from the receiver node to the transmitter node. In this time sensitive retransmission mechanism, if the packet is incorrect as before after one re-transmission, no more re-transmission request will be sent. And this packet will be abandoned and treated as a loss packet. And the expected transmission energy and the packet loss probability are provided as

$$p_{loss} = (1 - (1-p_e)^k)^2 = p_p^2 \tag{4.23}$$

$$\bar{E}_p = kE_b(p_p + 1) \tag{4.24}$$

where $\bar{E}_p$ denotes the expected transmission energy, and p_{loss} is the packet loss probability.

Case II*:* Certain Packet Loss Rate Re-transmission

In this scheme, the packet loss rate is required to be less than or equal to a certain value. And the packet will be retransmitted until the requirement is satisfied. This mechanism can be used to guarantee the service quality.

Number of retransmission: $\alpha = log_{p_p}\beta - 1$ (4.25)

Expected transmission energy: $\bar{E}_p = kE_b \frac{1-p_p^{\alpha+1}}{1-p_p}$, (4.26)

where α is the number of re-transmission, and β denotes the packet loss rate threshold.

Case III: Content Sensitive Re-transmission

In this mechanism, the re-transmission will be requested until the packet is correctly received. Some situations with a high requirement on the accurate data utilize this mechanism.

It is an extreme situation of the second case when the threshold of the packet loss rate, β →0 and the number of retransmission α →∞. The expected

Expected transmission energy: $\bar{E}_p = kE_b \frac{1}{1-p_p}$. (4.27)

4.5.2 Transmission with CPP Approach

According to the analysis on Coded Parity Packet presented in the previous section, it is clear that the CPP approach can reduce the packet error rate significantly. By using the associated parity packets, the packet error rate for a set of V source packets and E-V parity packets can be reduced to

$$p_{p-CPP} \approx (p_b)^{L_E}, \quad (4.28)$$

where p_b is the packet error rate for only one subset of associated parity packet is used in iterative soft decoding process [23]. And $L_E = 2^{V-E-1}$is introduce in section 5.3. On the other hand, the CPP approach reduces the packet error rate while increases the transmission energy on transmitting extra parity packets and redundant bits in Turbo coding which is not a small amount of energy. Therefore, CPP approach can greatly enhance the performance of the network and reduce the transmission energy by decreasing the number of re-transmissions when the signal to noise ratio is very low. However, when the signal to noise ratio is higher than a certain value which makes most of the packets can be received correctly without re-transmission, CPP approach is not necessary to adopted. The detailed analysis on when the CPP approach can be used to reduce the packet error rate and transmission energy at the same time is presented below.

For **Case I**:

If and only if the reduced packet error rate p_{p-CPP} by CPP scheme can satisfy the following formula, the CPP approach will reduce the transmission energy

$$kE_b(p_p + 1) \geq kE_b(p_{p-CPP} + 1)\frac{E}{rV}$$

$$\rightarrow p_{p-CPP} \leq \left(p_p + 1\right)\frac{rV}{E} - 1 \tag{4.29}$$

where r is the Turbo code rate which is less than one, p_p is the packet error rate of pure QAM packet without using CPP and re-transmission. The element, $\frac{E}{rV}$ indicates the ratio between whole bits, which includes the useful bits and redundant bits, and useful bits in CPP approach.

For **Case II**:

$$p_{p-CPP} \leq \frac{E(1-p_p)}{rV(1-p_p^{\alpha+1})} \tag{4.30}$$

For **Case III**:

$$p_{p-CPP} \leq 1\text{-}(1\text{-}p_p)\frac{E}{rV} \tag{4.31}$$

4.5.3 Transmission with Adjustable Power

If the transmission power raises from P to P', the bit error rate will be reduced which leads to a decrease in packet error rate. Let packet error rate becomes p'_p at power P'. If and only if the packet error rate p'_p satisfied the following inequalities at the transmission power P', the transmission energy will decrease.

For **Case I**:

$$\mathrm{P}(1+ p_p) \geq \mathrm{P'}(1+ p'_p)$$

$$\rightarrow p'_p \leq \frac{P(1+p_p)}{P'} - 1 \tag{4.32}$$

For **Case II**:

$$p'_p \leq 1 - \frac{P'(1-\mathrm{p_p})}{P(1-p_p^{\alpha+1})} \tag{4.33}$$

For **Case III**:

$$p'_p \leq 1 - \frac{P'(1-p_p)}{P} \tag{4.34}$$

4.5.4 An Adaptable Transmission Mechanism in Wireless Ad-Hoc Networks

In a wireless Ad-Hoc network, each data packet needs to be transmitted for *k* hops from the source node to the destination node. In this thesis, the incoming packet at each hop is assumed to be checked for error at the receiver. And the receiver will request a re-transmission, if the packet is detected erroneous. It leads to the packets content not error at the transmission node in each hop, and the re-transmission requests do not require going back to the previous hops.

Let's consider the multi-hop transmission of packet from node v_0 to v_n. v_1, v_2, …, v_{n-1} are n-1 intermediate relay nodes for transmission. The block diagram below illustrates the decision mechanism of v_i on receiving a data packet from its previous node v_{i-1} in the multi-hop transmission path.

When the packet from node v_{i-1} is received by v_i, v_i will first determine whether the received data is CPP encoded or not. If the packet is not CPP encoded, error detection process will be operated on the packet. If there are error being detected, a re-transmission request will be sent from node v_i to node v_{i-1}. If the packet is correct, this packet will be kept for later process. On the other hand, if the packet is CPP encoded, the node v_i will wait for the whole set of the CPP encoded packets which include *E* source packets and *V-E* associated parity packets and run CPP decoding process. If the source packets cannot be correctly decoded, a retransmission request will be sent from the node v_i to node v_{i-1}. Otherwise, the correctly decoded packets will be held for later process.

Then node v_i will determine whether it is necessary to use CPP for the next hop to node v_{i+1}. This decision is mainly based on the quality of the communication channel between node v_i and node v_{i+1} and the inequalities derived above. For instance, if the BER is high and the condition in inequalities (4.30) or (4.31) is satisfied, node v_i will decide to encode the packet by using CPP. Otherwise, node v_i will not adopt CPP scheme.

The last step is transmission power level selection. The lowest transmission power which satisfied inequalities (4) (5) (6) for different re-transmission schemes will be adopted in order to minimize the transmission energy.

The block diagram of the transmission scheme described above is illustrated in Figure 4.3.

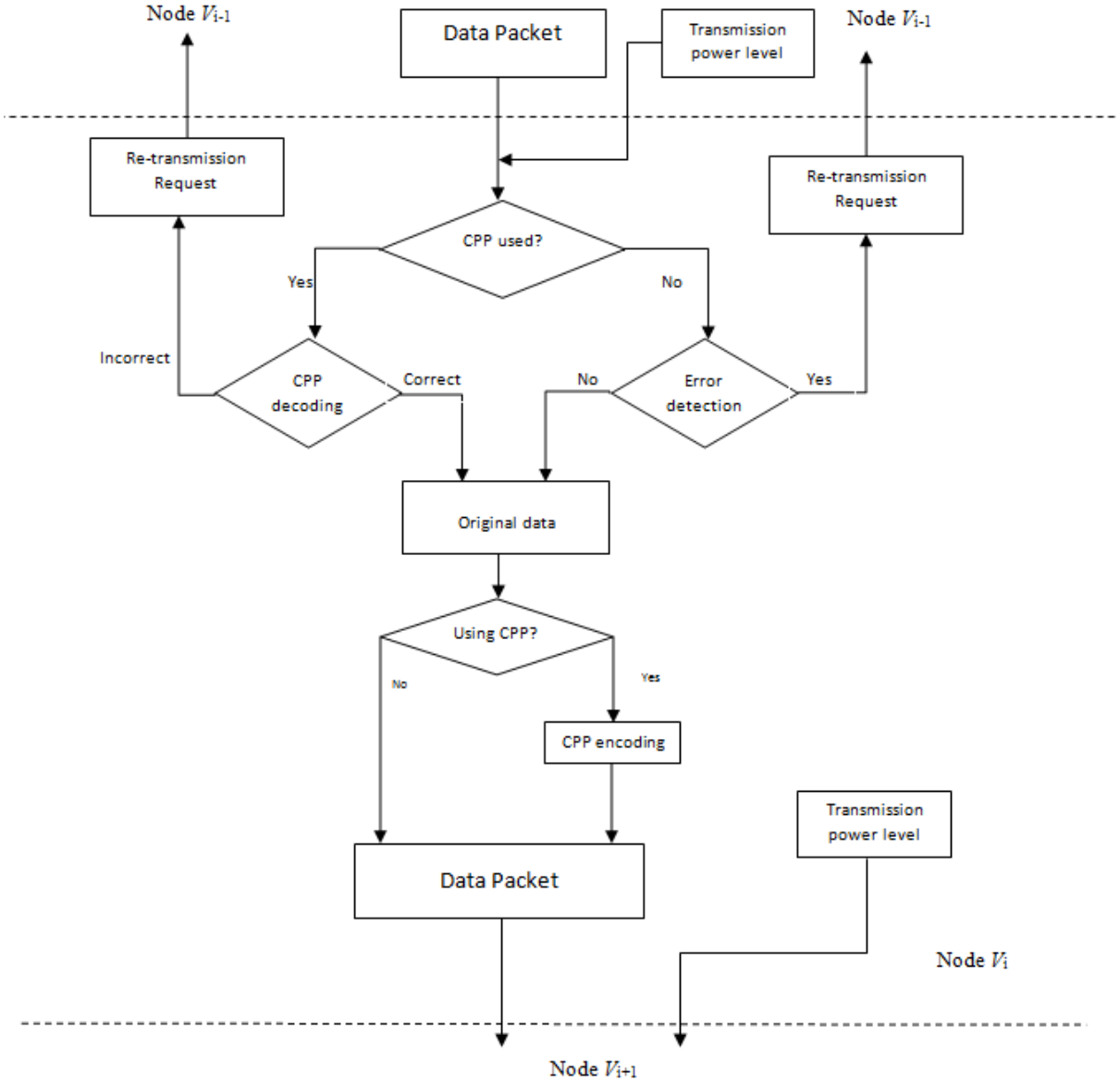

Figure 4.3 Flow chart of the adaptable transmission mechanism

4.6 Simulation and Performance Evaluation

Several simulations have been rum to observe the packet error rates, p_p for coded parity packet approach with various numbers of associated parity packets. Two groups of CPP approaches with different outer coder rate and inner coder rate are modulated with a 16-QAM scheme. In this simulation, the packet size is set to 84 bits. The effective data rate of the CPP scheme is given by

$$b = \frac{V}{E} r log_2 M \tag{4.35}$$

where V is the number of the source packet, E is the number of the source packets and the associated parity packets, r represents the Turbo coding rate which is called the inner code rate, and *M* denotes the constellation size [22].

In first set, the out code rate includes r_{out}=3/4, 3/5, 3/6, and the Turbo coding rate is r=1/2. The effective data rates of this set of schemes are 1.5 bits per symbol, 1.2 bits per symbol and 1 bits per symbol respectively. According to $L_E=2^{E-V-1}$, when r_{out} is ¾, there is only one set of the associated parity packet. And the numbers of the sets of the associated parity packets are 2 and 4 for r_{out}=3/5 and 3/6 respectively. The packet error rates for this set of the CPP schemes are illustrated in Figure 4.4. When SNR =3.75 dB, the packet error rates are 0.4198, 0.1638 and 0.0608 respectively. The packet error rate of CPP scheme with r_{out}=3/4 is the P_b in this case. Based on equation (4.28), the resultant $(P_b)^2$ and $(P_b)^4$ are 0.1762 and 0.0311, which are close to the simulation results. From the Figure 4.4, it is clear that when the number of source packet is given, the set with more associated parity packets provides a lower packet error rate. And when the CPP approach is adopted, the packet error rate has been reduced significantly as compared with the packet without using CPP scheme.

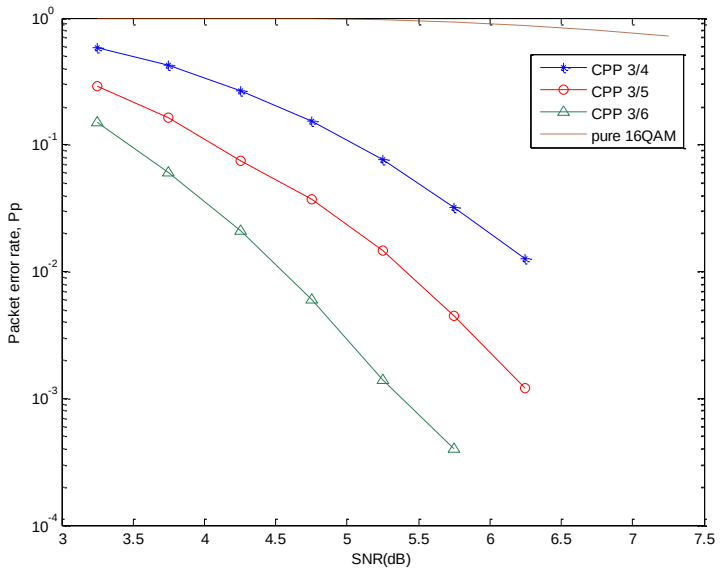

Figure 4.4 The packet error rate for the first set of CPP code rates

As mentioned in section 4.3.1, there are two ways to increase the number of the associated parity packet sets L_E which are increasing α and increasing the number of the parity packets. A simulation has been run to test and analyze these two methods. The results are plotted in Figure 4.5. In this simulation, the outer code rates are given as 4/6, 6/9 and 4/7, and the inner code rate is set at 3/4. A 16-QAM scheme is adopted. According to equation (4.35), the

effective code rates of these three approaches are 2 bits per symbol, 2 bits per symbol and 1.71 bits per symbol respectively. It is observed that the CPP approach with an outer code rate 4/6 has the largest packet error rate among three approaches. And the other two approaches' packet error rates are close to each other. The CPP approach with V/E=6/9 utilizes the method of increasing α. It can be inspected that $\frac{V}{E} = \frac{\alpha V_0}{\alpha E_0} = \frac{\frac{3}{2}\times 4}{\frac{3}{2}\times 6} = \frac{6}{9}$ and α=1.5 in this case. And the number of parity packet sets increases from L_E=2 to L_E=4 which leads to the decrease in packet error rate. The last approach with V/E=4/7 is just simply adding one more associated parity packet based on the approach with V/E=4/6. And the number of associated parity packet sets increases from L_E=2 to L_E=4 as well. It can be observed that the performances of these two methods in this case are similar to each other, and they can both reduce the packet error rate of the approach with V/E=6. It should be note that there is an unsmooth change in the case of V/E=6/9 when SNR is 9.25 dB. It is because the packet error rate is too small and the number transmission and receiving packets is not large enough to accurately measure it. Therefore, in order to achieve more accurate results, more packets should be simulated to estimate the packet loss rate when SNR increases.

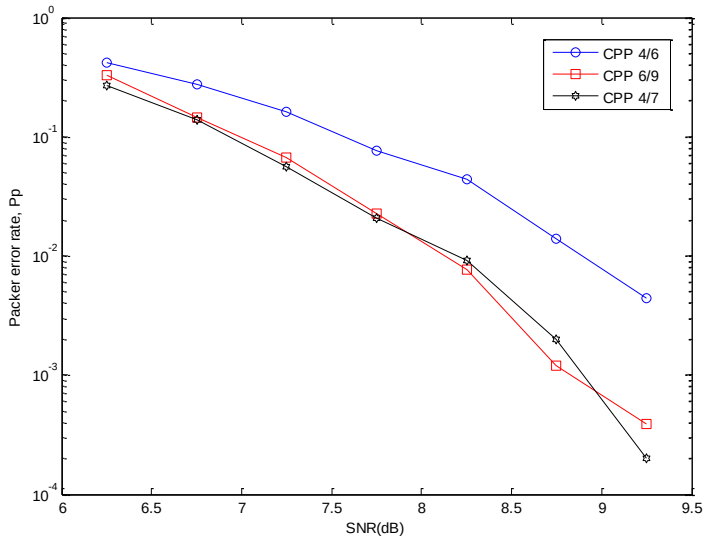

Figure 4.5 The packet error rate of the second set of the CPP code rates

According to the brown line in Figure 4.4, it is obvious that the packet error rate is extremely high without adopting CPP approach when SNR is less than 10 dB. The communication cannot even fulfil in a channel with such a high packet error rate. However, the packet error rates of the CPP approaches are relatively low. Therefore, CPP scheme can be adopted to accomplish successful transmission and receiving in channels with very low

SNR. The performance of the adaptable transmission mechanism, which is developed in section 4.6, is analysed below. The simulation has been run between packets adopting CPP approach with $r_{out} = \frac{3}{4}, r_{in} = 1/2$ and packets without any channel coding under the content sensitive re-transmission scheme (Case III). By equation (4.31), it has been shown that when SNR is lower than 7.65 dB, using this specific CPP approach will reduce number of retransmission and save the transmission energy. While SNR exceeds 7.65 dB, though this CPP approach can reduce the packet error rate, but the energy used on the redundant bits, such as the bits in parity packets and turbo codes, are even greater than the energy used on re-transmission. Therefore, by utilizing equation (4.29)-(4.34), CPP approach can be appropriately implemented in wireless Ad-Hoc networks according to the various channel conditions in different hops. And this adaptable transmission mechanism has the potential to contribute several benefits to the wireless Ad-Hoc networks:

1) Short end-to-end delay. As the CPP approach is appropriately adopted, the packet error rate and the number of retransmission can both be reduced.
2) High energy efficiency. It is because this mechanism can choose the best channel code scheme with the least expected transmission energy according to the channel condition.

Chapter 5

Summary and Future Work

This chapter presents a brief summary of this thesis, and also addresses several areas that some further research can focus on.

5.1 Thesis Summary

This thesis investigates on the resource allocation in wireless Ad-Hoc networks, and it focuses on the physical and MAC layers. The key contributions of this thesis are the development of an energy-aware routing path discovery algorithm and the invention of an adaptable transmission mechanism, which are both used to realize the energy efficiency communication in wireless Ad-Hoc networks.

In this thesis, the problem of the inefficient energy allocation in the current HSDPA systems is addressed. In order to solve this problem, the two-group resource allocation scheme is proposed with adaptive channels to utilize the residual energy. Depends on the received SNR, this algorithm can allocate the data bits into two groups of parallel channels which have different modulation schemes. From the results, this approach is examined to reduce the residual energy significantly in both interference-free channels and interference-existing channels. And an extended chip sampling window is introduced to incorporate the inter-symbol interference in multipath channels. Moreover, the data rate achieved by the two-group resource allocation scheme is closer to the system capacity in HSDPA systems.

After the resource allocation schemes are studied and simulated to achieve the energy efficient transmission in HSDPA systems at the physical layer, this thesis then investigates in the energy-aware routing path discovery schemes which consider the data rate and the energy consumption per bit for each hop as the cost function. At first, a trellis-hop diagram approach is presented to find all the possible paths for a pair of nodes. However, this scheme has an extremely high computational complexity. Then a modified Viterbi algorithm is proposed to reduce the computational complexity of the routing path discovery process for a given pair of

node by choosing the link-joint routing path with the minimum cost while abandoning the other link-joint routing paths. However, as both of these two algorithms are not computational efficient to find the best routing paths for all-pair of nodes in a network, a modified Floyd's algorithm is developed to solve this problem in this thesis.

After the energy efficient HSDPA system is implemented on each wireless hop link and the multiple routing paths between the source node and the destination node are constructed in a wireless Ad-Hoc network, DCF service time at the MAC layer is investigated in. By studying and modelling the Carvalho model, the throughput and end-to-end delay improvements achieved by the two-group resource allocation scheme is presented and analysed.

Finally, the thesis studied the coded parity packets approach and developed an adaptable transmission mechanism for wireless Ad-Hoc networks. From the results, and coded parity packet approach can reduce the packet error rate and the number of retransmissions significantly. And the adaptable transmission mechanism, which can make appropriate decisions on using the coded parity packets scheme or not, can short the end-to-end delay time and achieve the energy efficient communication in wireless Ad-Hoc networks.

5.2 Future Work

Several areas, which are worth to be further investigated in, are listed below.

1) Extending the topology to 3 dimensions.

As the propagation loss model is concerned with the heights of transmitting and receiving antennas, the differences in terrain elevations can be taken into consideration in this project. Moreover, in reality the sensors are distributed randomly in a certain range with different terrain which can make differences between antenna heights, it must cause a certain effect in propagation loss.

2) Adopting directional antennas

As the hop links suffer from the propagation loss greatly, adopting directional antenna in each node can increase the efficiency of the network. And according to [8], the end-to-end delay can also be reduced by implementing the directional antennas.

3) Consider energy constraint in network layer

By considering the energy constraint and the resource allocation scheme, an Energy Aware AODV can be developed. As the exponent of propagation loss is more than 2, the total transmission energy of multi hop route is often smaller than the direct route. Therefore, in EAAODV protocol, the energy consumed per bit is determined by using two-group resource allocation scheme, and then the multi hop routes with less energy utilization are chosen as the best route. However, it is not that easy to make it happen. Because the multi hop route has a longer end-to-end delay than the direct route. It means that the RREQ with the less hop counts reaches the destination first, and then this path will be encapsulated in the packet RREP and sent back to the source even before the other RREQ reaching the destination. To solve this problem, the RREQ with the less hop counts should be delayed.

4) Adopting NS2 to examine the results

In this thesis, the proposed resource allocation scheme at MAC layer is only tested in the network scenarios designed in MATLAB. More accurate simulation results are expected to be acquired from the network simulator, such as NS2.

REFERENCE

[1] Krunz, M.; Muqattash, A.; Sung-Ju Lee; "Transmission power control in wireless ad hoc networks: challenges, solutions and open issues", *Network, IEEE* Volume: 18 , Issue: 5 , 2004 , Page(s): 8 – 14.

[2] A. Goldsmith, Wireless Communications, *Cambridge*, 2005.

[3] C.K. Toh, Ad Hoc Mobile Wireless Networks: Protocols and Systems, *Prentice Hall*, Dec. 2001.

[4] C. E. Perkins, P. Bhagwat, "Highly Dynamic Destination-Sequenced Distance Vector (DSDV) for Mobile Computers", *Proc. of the SIGCOMM 1994 Conference on Communications Architectures, Protocols and Applications*, Aug 1994, pp 234-244.

[5] Optimized Link State Routing Protocol (OLSR), http://tools.ietf.org/html/rfc3626.

[6] M. Marina, S. Das, "On-demand Multipath Distance Vector Routing in Ad Hoc Networks", *Proceedings of the 2001 IEEE International Conference on Network Protocols (ICNP)*, pages 14--23, IEEE Computer Society Press, 2001.

[7] David B. Johnson, David A. Maltz, Thomasz Imielinski and Hank Korth (Editors), "Dynamic Source Routing in Ad Hoc Wireless Networks", *Mobile Computing*, Vol. 353, Chapter 5, pp. 153-181, Kluwer Academic Publishers, 1996.

[8] P. Appavoo and K. Khedo, Sencast, "A Scalable Protocol for Unicasting and Multicasting in a Large Ad hoc Emergency Network", *International Journal of Computer Science and Network Security*, Vol.8 No.2, February 2008.

[9] Khelifa, S.; Maaza, Z.M.; "An Energy Multi-path AODV Routing Protocol in Ad Hoc Mobile Networks", *5th International Symposium on Communications and Mobile Network (ISVC)*, Page(s): 1 – 4, 2010.

[10] Tai Hieng Tie; Chong Eng Tan; Sei Ping Lau; "Alternate Link Maximum Energy Level Ad Hoc Distance Vector Scheme for Energy Efficient Ad Hoc Networks Routing", *2010 International Conference on Computer and Communication Engineering (ICCCE)*, pp. 1 – 6, 2010.

[11] Marwan Krunz , Alaa Muqattash , Sung-ju Lee, "Transmission power control in wireless ad hoc networks: challenges, solutions, and open issues*", IEEE Network*, vol. 18, Issue: 5, pp. 8-14, 2004..

[12] Juan-Carlos Cano and Pietro Manzoni, "A Performance Comparison of Energy Consumption for Mobile Ad Hoc Network Routing Protocols," *Eighth International Symposium on Modeling, Analysis and Simulatio of Computer and Telecommunication Systems (MASCOTS 2000),* Aug 2000.

[13] Xiaoqin Wang and Jinping Hao, "A Hybrid Propagation Model Using the Detailed Irregularities Terrain Profile Data", *Proc. of International Conference on Signal and Information Processing (ICSIP) 2010,* China, Dec. 2010.

[14] T. S. Rappaport. Wireless communications, principles and practice. *Prentice Hall,* 1996.

[15] He, Z. (2010) Efficient Radio Resource Allocation Schemes and Code Optimizations for High Speed Downlink Packet Access Transmission. PhD's Thesis. Imperial College London.

[16] "HSPA mobile broadband today", http://www.gsmamobilebroadband.com/.

[17] 3GPP, 3GPP TR 25.828: High Speed Downlink Packet Access: Physical Layer Aspect, v5.0.0 ed., March 2002.

[18] J. Zhou and M. K. Gurcan, "An Improved Multicode CDMA Transmission Method for Ad Hoc Networks", *IEEE Wireless Communications & Networking Conference 2009 (WCNC2009),* Budapest, Hungary, 5-8 April 2009.

[19] M. M. Carvalho and J. J. Garcia-Luna-Aceves, "A Scalable Model for Channel Access Protocols in Multihop Ad Hoc Networks*", ACM Mobicom*, Pennsylvania, 2004.

[20] J. Zhou, M. K. Gurcan, and A. Chungtragarn, "Energy-aware Routing with Two-group Allocation in Ad Hoc Networks", *the 25th International Symposium on Computer and Information Sciences*, The Royal Society, London, United Kingdom, 22-24 September 2010.

[21] M. K. Gurcan, H. Ab Ghanai, J. Zhou, and A. Chungtragarn, "Bit Energy Consumption Minimization for Multi-path Routing in Ad-hoc Networks", *the Computer Journal*, Oxford University Press, January 2011.

[22] Gurcan, M.K.; Ab Ghani, H.; "small-sized packet error rate reduction using coded parity packet approach", *2010 IEEE 21st International Symposium on Personal Indoor and Mobile Radio Communications (PIMRC)*, page(s): 419 – 424, 26-30 Sept. 2010.

[23] M. K. Gurcan and Hadhrami Ab. Ghani, "Coded Parity Packet Approach for Small-sized Packet Transmission in Wireless Ad-hoc Networks", *European Transactions on Telecommunications*. 2010.

[24] Zhou, J. (2010), "Resource Allocation in Ad Hoc Networks", PhD's Thesis. Imperial College London.

[25] Z. He and M. Gurcan, "Optimized resource allocation of hsdpa using two group allocation in frequency selective channels," in *IEEE WCSP 2009*, (Nanjing, China), November 2009.

[26] Z. He and M. K. Gurcan, "Optimizing radio resource allocation in hsdpa using 2 group allocation," in *IWCMC '09: Proceedings of the 2009 International Conference on Wireless Communications and Mobile Computing*, (New York, NY, USA), pp. 1107–1111, ACM, 2009.

[27] Hadhrami Ab. Ghani, M.K. Gurcan and Zhengfeng He, "Two-Group Resource Allocation with Channel Ordering And Interference Cancellation", *IEEE WCNC 2010.*

[28] "IEEE 802.11 Standard", http://standards.ieee.org/getieee802/download/802.11-2007.pdf

[29] G. Bianchi, "Performance analysis of the IEEE 802.11 distributed coordination function," *IEEE Journal on Selected Areas in Communications*, vol. 18, no. 3, pp. 535-547, March 2000.

[30] M. M. Carvalho and J. J. Garcia-Luna-Aceves, "Delay analysis of IEEE 802.11 in single-hop networks," in *Proc. of 11th IEEE International Conference on Network Protocols (ICNP)*, Atlanta, USA, November 2003.

[31] Destounis, A. (2010) On HSDPA Femtocell Technology for ad hoc and wireless sensor networks: investigation of the routing problem. Master's Thesis. Imperial College London.

[32] Weisstein, Eric. "Floyd-Warshall Algorithm". Wolfram MathWorld. http://mathworld.wolfram.com/Floyd-WarshallAlgorithm.html.

[33] Dequan Zhang, Guolin Wu, "Optimization of Floyd Algorithmic for Shortest Path Problem", *Journal of Xuchang University*, Vol. 28, 2009.

[34] Axler, Sheldon (February 26, 2004), Linear Algebra Done Right (2nd ed.), Springer, ISBN 978-0387982588.

[35] Shannon C, "A mathematical theory of communications", *Bell Systems Technical Journal* 1948; 27:379–423, 623–656.

[36] M. S. Raju, R. Annavajjala, and A. Chockalingam, "BER Analysis of QAM on Fading Channels with Transmit Diversity," *IEEE Transactions on Wireless Communications*, vol. 5, no. 3, pp. 481–486, March 2006.

[37] Poor HV, "Wireless Communication Systems: Advanced Techniques for Signal Reception", Prentice Hall, 2003.

[38] Hagenauer J, Offer E, Papke L., "Iterative decoding of binary block and convolutional codes", *IEEE Transactions on Information Theory*, March 1996; 42(2):429–445, doi:10.1109/18.485714.

[39] Sankarasubramaniam, Y.; Akyildiz, I.F.; McLaughlin, S.W., "Energy efficiency based packet size optimization in wireless sensor networks", *Proceedings of the 2003 IEEE International Workshop on Sensor Network Protocols and Applications*, page(s): 1 – 8, 2003.